Fullerene Chemistry

DOI: 10.1002/anie.200901746

Chemical, Electrochemical, and Structural Properties of Endohedral Metallofullerenes

*Manuel N. Chaur, Frederic Melin, Angy L. Ortiz, and Luis Echegoyen**

Keywords:
electrochemistry · electronic properties · endohedral fullerenes · molecular electronics

Dedicated to Professor Jean-Marie Lehn on the occasion of his 70th birthday

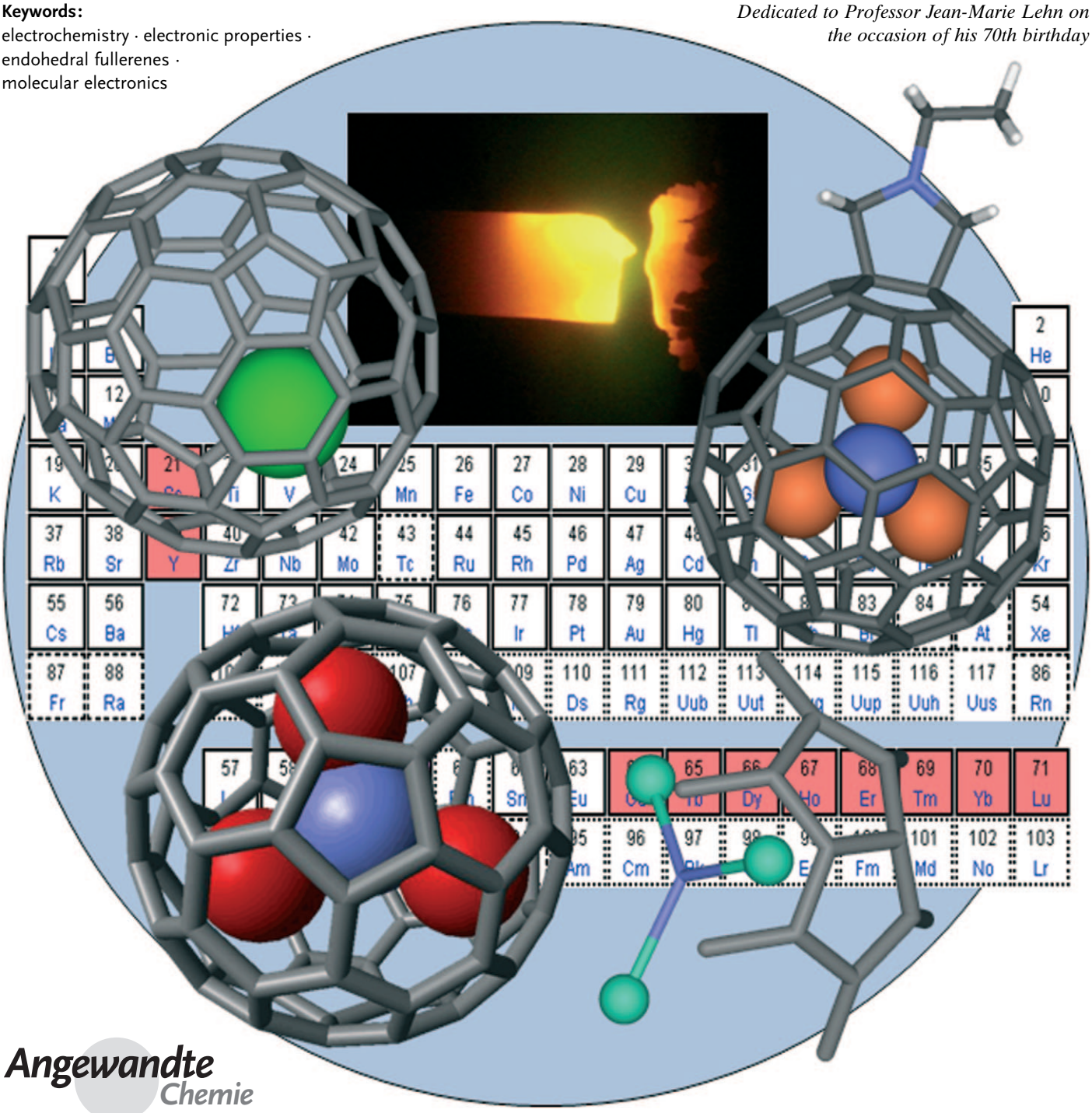

Ever since the first experimental evidence of the existence of endohedral metallofullerenes (EMFs) was obtained, the search for carbon cages with encapsulated metals and small molecules has become a very active field of research. EMFs exhibit unique electronic and structural features, with potential applications in many fields. Furthermore, functionalized EMFs offer additional potential applications because of their higher solubility and their ease of characterization by X-ray crystallography and other techniques. Herein we review the general field of EMFs, particularly of functionalized EMFs. We also address their structures and their (electrochemical) properties, as well as applications of these fascinating compounds.

From the Contents

1. Introduction

From the early stages of fullerene research it was shown that fullerenes were in general able to host atoms and even small molecules in their interior.[1] Even though lanthanum was the first metal to be successfully encapsulated inside carbon cages, other metals have been also caged, mainly from groups II and III, all the lanthanides as well as their corresponding metallic nitride clusters, metallic carbides, noble gases, phosphoros, nitrogen, and even metal oxides.[3–13] The search to encapsulate metals, metal clusters, and small molecules inside fullerenes has been driven not only by curiosity but also because EMFs offer a broad range of properties that could be of fundamental use in different fields, such as materials science and medicine. For example, gadolinium EMFs have been widely studied because of their magnetic contrast-enhancing properties.[8,14,15] The highly paramagnetic and radioactive character of some EMFs endows them with potential applications in medicine.[16–19] On the other hand, their low HOMO–LUMO gaps as well as their electronic properties can be exploited in molecular electronics and electron donor/acceptor systems.[6,8,20–26]

As noted from the beginning of research into metallofullerenes, EMFs exhibit interesting and intriguing electronic properties, which are explained by electron transfer from the encapsulated moiety to the carbon cage.[2–9,27] This electron donation makes possible the encapsulation of very unstable moieties that have never been independently isolated.

It is well known that fullerenes tend to follow the isolated pentagon rule (IPR); thus, fullerenes with adjacent pentagons have a higher formation energy than those with isolated pentagons.[28] While no exception to this rule has ever been reported for empty fullerenes, it turns out that this rule becomes more of a suggestion when considering EMFs, since several non-IPR carbon cages that encapsulate metallic moieties have been prepared and characterized.

The chemical functionalization of EMFs is a key step in the development of these compounds for potential applications.[29] The first EMF derivative was reported in 1995 by Akasaka et al., where La@C_{82} was photochemically induced to react with disilirane.[30a] Besides photochemical reactions other types of reactions have been reported, including Diels–Alder, 1,3-dipolar cycloadditions, Bingel–Hirsch, free radicals, and other addition reactions.[29–90] Exohedral functionalization of EMFs has provided the opportunity to characterize different metallofullerenes, since functionalized EMFs are relatively easier to crystallize than their unfunctionalized precursors.[36–37,39,75] Furthermore, the addition of water-soluble groups to EMFs have made it possible to study their properties in biological systems.[14–19]

Other reviews have addressed the synthesis of classical EMFs and metallic nitride EMFs,[2–9] so herein we discuss their synthesis and purification in a general manner, concentrating on the most interesting electronic/structural features of EMFs, primarily those involving violations of the IPR rule. The main focus is on non-IPR structures, metallic carbides and metallic nitride EMFs. For the first time, the chemical properties of EMFs and their electrochemical properties are reviewed. Finally, we will focus on applications.

2. Synthesis and Purification of EMFs

The first proposal of an endohedral metallofullerene was given only days after the discovery of C_{60} by Kroto et al.[91] Kroto and co-workers found a series of C_n^+ and LaC_n^+ ions in the mass spectrum of a sample prepared by the vaporization of graphite rods impregnated with $LaCl_2$.[1] However, the large-scale production of C_{60} and EMFs was not accomplished until 1990, when Krätschmer et al. successfully synthesized C_{60} by resistive heating of graphite rods in a helium atmosphere.[92] Since then, many methods for the production of EMFs have been reported;[2–9] the most common method is the modified arc-discharged Krätschmer–Huffman reactor. In

[*] M. N. Chaur, A. L. Ortiz, Prof. Dr. L. Echegoyen
Department of Chemistry, Clemson University
219 Hunter Laboratories, Clemson, SC 29631-0973 (USA)
Fax: (+1) 864-656-6613
E-mail: luis@clemson.edu
Dr. F. Melin
Laboratoire de Spectroscopie Vibrationnelle et Electrochimie des Biomolecules, Faculte de Chimie
1 Rue Blaise Pascal, 67070 Strasbourg (France)

this synthesis process, graphite rods are packed with the desired metal oxide (or a combination of metal oxides if mixed EMFs are wanted), and then the packed rods are annealed over several hours before finally being burned in the presence of He or Ar.[2–9]

In the synthesis of metallic nitride (MN) EMFs, a nitrogen source is added, commonly, nitrogen or ammonia.[93,94] The former synthesis method—termed the trimetallic nitride template (TNT) method—was discovered by Dorn and co-workers during the synthesis of the first metallic nitride EMF ($Sc_3N@C_{80}$) in 1999.[93] The second, most traditional, method for the synthesis of metallic nitride EMFs is the "reactive gas atmosphere" introduced by Dunsch and co-workers, where ammonia is used as a reactive gas. With this method, metal nitride EMFs were synthesized for the first time almost exclusively with less than 5% empty fullerenes.[94] Other synthetic methods include the use of solid sources of nitrogen, but these methods afford lower yields of EMFs and are not reproducible.[7–9] Figure 1 shows a simple sketch of an arcing reactor for the synthesis of EMFs. More sophisticated arc reactors have enabled anaerobic collection and sampling.

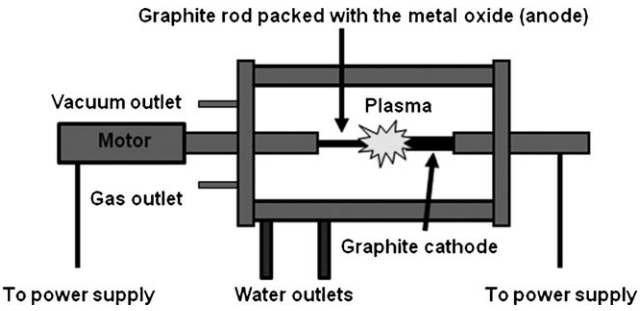

Figure 1. Arc-discharge reactor for the production of fullerenes. The gas atmosphere can be regulated depending on the type of EMFs desired.

2.1. *Families of EMFs*

Endohedral fullerenes can be divided into several classes:

- classical EMFs ($M@C_{2n}$ and $M_2@C_{2n}$, M = metal and $60 \leq 2n \leq 88$),
- metallic carbide EMFs ($M_2C_2@C_{2n}$ and $M_3C_2@C_{2n}$, M = metal and $68 \leq 2n \leq 92$),
- metallic nitride EMFs ($M_3N@C_{2n}$, M = metal and $68 \leq 2n \leq 96$),
- metallic oxide EMFs ($M_4O_2@C_{80}$).

The symmetry and structures of most of these EMFs have been successfully characterized by NMR spectroscopy and X-ray diffraction. The latter method is especially important for those EMFs with paramagnetic metals or clusters. In the case of metallofullerenes for which no X-ray analysis is available, IR and Raman spectroscopy supported by DFT calculations have provided valuable information.[2,7,8]

2.1.1. *Classical EMFs*

As mentioned before, Kroto and co-workers first proposed the existence of an endohedral metallofullerene in 1985;[1] however, it was not until 1995 that the first structural characterization of an EMF (by synchrotron powder X-ray diffraction (XRD) and the maximum entropy method (MEM)/Rietveld analysis) was reported.[95] Since then, many EMFs with up to four encapsulated metals have been isolated and characterized by mass spectrometry (MS), UV/

Manuel N. Chaur was born in 1984 in Cali, Colombia. He received his BSc in Chemistry from the Universidad del Valle in 2006. In 2005, he completed a research project under the guidance of Prof. S. Stuart, working on molecular dynamic simulations of carbon structures. He is currently carrying out PhD research under the supervision of Prof. Luis Echegoyen at Clemson University. His work involves the synthesis and electrochemical characterization of EMFs.

Frederic Melin was born in 1976 near Paris, France. He received his PhD from the Université de Strasbourg in 2005. After post-doctoral studies with Prof. Luis Echegoyen, he accepted a "Maître de Conférences" position in Strasbourg. His main research interests are the electrochemistry of fullerenes, porphyrins, and proteins.

Angy L. Ortiz was born in Cali, Colombia in 1982. In 2004, she received her BS in Chemistry from the Universidad del Valle in Colombia. After a research project at Clemson University, in 2006 she began PhD research in the group of Prof. Luis Echegoyen. Her current research interests are the design and regioselective synthesis of two- and three-pronged C_{60} fullerene derivatives and their applications in molecular electronics.

Prof. Luis Echegoyen was born in La Habana, Cuba, in 1951. He obtained both his BSc and PhD from the University of Puerto Rico in Rio Piedras (1971 and 1974, respectively). After an industrial placement at Union Carbide and several professorships at the Universities of Puerto Rico, Maryland, and Miami, in 2002 he was appointed as Chair of the Department of Chemistry at Clemson University, in South Carolina. His research interests include fullerene chemistry, electrochemistry, and supramolecular chemistry, with special emphasis on molecular electronics and endohedral fullerenes.

Vis-NIR spectroscopy, cyclic voltammetry (CV), electron energy loss spectroscopy (EELS), electron paramagnetic resonance (EPR), density functional theory (DFT) calculations, NMR spectroscopy, XRD measurements, and some other characterization techniques.[2–8]

As reviewed before,[2–6] the most abundant classical EMF family is the $M@C_{82}$ species, the first example being $La@C_{82}$, followed by $Y@C_{82}$, $Sc@C_{82}$, and encapsulated lanthanides inside C_{82}.[2–6] The chemical functionalization and electrochemical properties of these EMFs will be reviewed in Section 3.

2.1.2. Metallic Carbide EMFs

Metallic carbide EMFs are a special type of fullerenes that encapsulate a metallic carbide moiety in their interior (Figure 2). The first structural characterization of a metallic

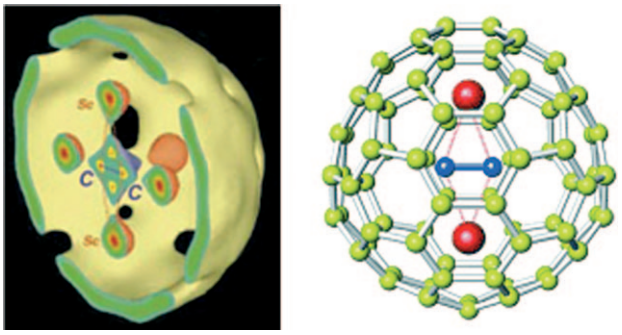

Figure 2. Left: Half section of the equicontour (1.9 e Å^{-3}) surface of the MEM charge density for $Sc_2C_2@C_{84}$. Right: Structure of $Sc_2C_2@C_{84}$ (based on synchrotron powder diffraction spectrocopy and ^{13}C NMR spectroscopy).[96]

carbide EMF was reported in 2001 by Shinohara et al.[96] Both ^{13}C NMR and synchrotron X-ray structural analyses were used to determine the endohedral character of the Sc_2C_2 unit inside the C_{84}-D_{2d} carbon cage.[96] The same metallofullerene had previously been isolated by the same research group, but they erroneously assigned it as $Sc_2@C_{86}$ (isomer I).[97] In a similar way, theoretical calculations as well as ^{13}C NMR spectroscopy and refined X-ray structural analyses have revealed over the past years other metallic carbide EMFs such as $Y_2C_2@C_{82}$ (isomers C_s, C_{2v}, and C_{3v}), $Ti_2C_2@C_{78}$ (D_{3h}), $Sc_2C_2@C_{68}$ (C_{2v}), $Sc_2C_2@C_{82}$ (C_{3v}), $Sc_3C_2@C_{80}$ (I_h), and $Gd_2C_2@C_{92}$ (D_3).[36,37,98–106] Interestingly, among all of these EMFs, only $Sc_2C_2@C_{68}$ (C_{2v}) was found to have a non-IPR carbon cage.[104]

Crystallographic data together with calculations have strongly suggested that the metallic carbide unit is more stable in the bent geometry. In this conformation the carbon–carbon bond in $Sc_2C_2@C_{82}$ (C_{3v}) was measured to be 0.127 nm, which corresponds to two carbon atoms connected through a triple bond.[37] By using ^{13}C-enriched samples, Nagase and co-workers reported the chemical shifts of several metallic carbide EMFs.[107] The chemical shifts of the C_2 unit were found at $\delta = 249.2$, 253.2, and 328.3 ppm for $Sc_2C_2@C_{84}$ (D_{2d}), $Sc_2C_2@C_{82}$ (C_{3v}), and $[Sc_3C_2@C_{80}]^-$ (I_h), respectively. Such low-field resonances were explained by the presence of the two Sc^{3+} ions and the dianionic character of the C_2 unit.

A special type of metallic carbide EMF is $Sc_3C_2@C_{80}$,[36] being the first and only metallic carbide EMF isolated to date with three metals in the endohedral cluster. When first reported in 1994, the EPR spectrum of this EMF showed well-resolved hyperfine splitting, with 22 equally spaced peaks arising from the equivalency of the three Sc metals inside the carbon cage.[108] However, in 2005 Nagase and co-workers reported the chemical functionalization of this EMF and found that it was actually a metallic carbide.[36]

The electronic structure of metallic carbide EMFs such as $M_2C_2@C_{82}$ was studied by Poblet and co-workers.[109] They proposed that empty cages with a large (LUMO−3)-(LUMO−2) gap are more suitable for encapsulating the M_2C_2 moiety because of the stabilization obtained by the formal transfer of four electrons from the cluster to the LUMO−1 and LUMO−2 of the carbon cage. This methodology suggested that isomer 85 in which the C_{92} empty fullerene with D_3 symmetry would be energetically more favored to host the M_2C_2 cluster, and this was confirmed for $Gd_2C_2@C_{92}$ (D_3).[106]

2.1.3. Metallic Nitride EMFs

These relatively new compounds, discovered only ten years ago, are undoubtedly among the most interesting EMFs. The quite high yield of $Sc_3N@C_{80}$, as reported by Dorn and co-workers,[93] emphasized the stabilization provided by the electron transfer between the internal cluster and the carbon cage. Neither the metallic nitride cluster nor the C_{80}-I_h carbon cage have been prepared independently. However, when associated together they form a very stable compound, which can be obtained in even higher yields than the empty C_{84} carbon cage, which was considered until then as the third most abundant fullerene obtained during the arcing process.[93] The synthesis of scandium nitride EMFs also allows the formation of carbon cages with smaller size, such as $Sc_3N@C_{68}$ and $Sc_3N@C_{78}$, as well as the two isomers of $Sc_3N@C_{80}$, the I_h symmetric one, which is the major product and the D_{5h} isomer.[7–9,93,110]

It has been shown experimentally and theoretically that the metallic nitride cluster donates six electrons to the carbon cage. Poblet and co-workers rationalized the formation of $Sc_3N@C_{68}$, $Sc_3N@C_{78}$, and $Sc_3N@C_{80}$ on this basis, and demonstrated that only certain carbon cage isomers have the most favored molecular orbital distribution to accommodate the incoming electrons.[111] Possible host cages for metallic nitride clusters were also predicted from this model by generalizing a rule of stabilization that states that only fullerenes with a large enough (LUMO + 3)-(LUMO + 4) gap would be suitable to accommodate the metallic nitride cluster. Popov and Dunsch extensively analyzed the structures of larger metallic nitride EMFs on the basis of the stability of fullerenes in their hexaanionic state, and they were able to predict the symmetry of metallic nitride EMFs, which were later confirmed experimentally.[112]

Recently, metallic nitride EMFs have been prepared with metals from group III and lanthanides either as homogenous

metallic nitride EMFs or as mixed metallic nitride EMFs. A wide cage-size distribution is usually observed, from C_{68} to C_{104}.[7–9,93,113,114] As a consequence of its very low ionic radius, scandium forms a small cluster nitride that fits perfectly inside the C_{80} (I_h) cage, and this favorable fit along with the stabilization resulting from the electron transfer from the cluster to the carbon cage makes $Sc_3N@C_{80}$ the most common EMF prepared so far.[7–9,93] When the ionic radius of the metal is increased, the yield of the EMFs is considerably decreased, but the C_{80} cage is still favored. However, a different tendency is observed beyond gadolinium: As the ionic size of the metal increases, the yield slightly increases again and neodymium, praseodymium, and cerium are preferentially encapsulated as metallic nitrides inside the C_{88} carbon cage, while lanthanum nitride is preferentially encapsulated inside the C_{96} cage (Figure 3).[113,114] The mass spectra of the $La_3N@C_{2n}$ family

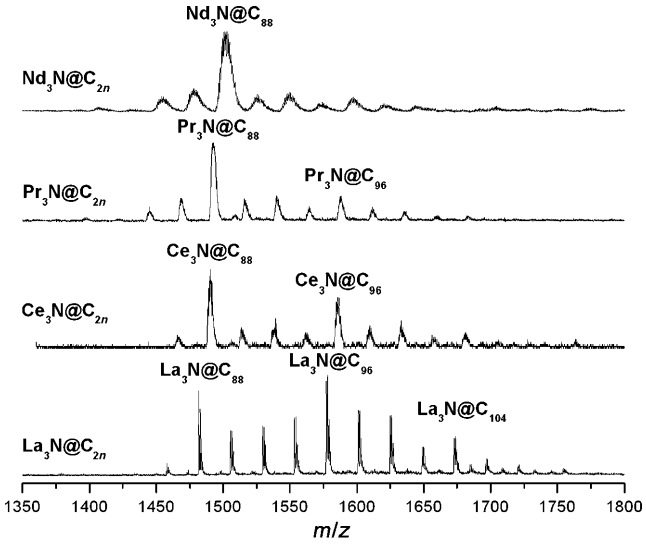

Figure 3. Mass spectra of the Nd, Pr, Ce, and La metallic nitride EMFs and their fullerene cages.

shows that after C_{96}, the most abundant cage corresponds to C_{104}. It is interesting to note that the preferentially templated cages seem to increase in size by eight carbon atoms as the size of the internal cluster increases. So far, the nature of this discrete increase is not understood.[9,113]

2.1.4. *Metallic Oxide EMFs*

Stevenson et al. recently reported the synthesis of an EMF encapsulating a metallic oxide cluster consisting of six atoms, $Sc_4(\mu_3\text{-}O)_2@C_{80}$ (I_h), by vaporizing graphite rods packed with scandium oxide in the presence of helium and a small amount of air. The yield of this compound was increased considerably by the addition of copper nitrate in the packed rods. High-resolution mass spectrometry revealed the presence of two other metallic oxide EMFs with the general formulas $C_{80}O_2Sc_4$ and $C_{80}O_3Sc_4$. Figure 4 shows the structure of $Sc_4(\mu_3\text{-}O)_2@C_{80}$ (I_h) obtained from crystallographic data.[10]

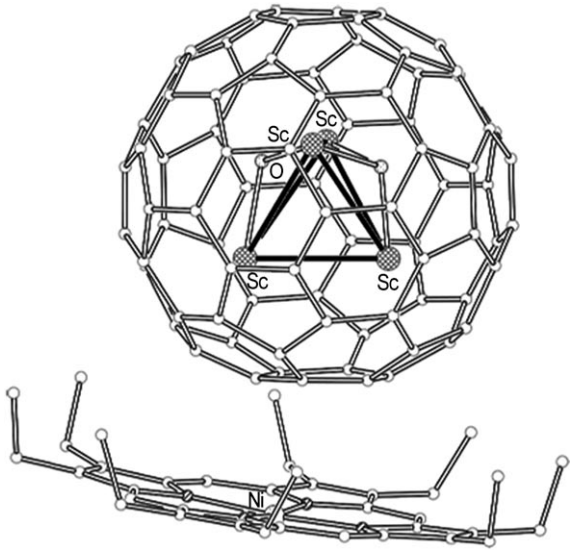

Figure 4. Structure of the metallofullerene $Sc_4(\mu_3\text{-}O)_2@C_{80}[I_h]\cdot Ni^{II}(OEP)\cdot 2C_6H_6$ (OEP = octaethylporphyrin). Reproduced with permission from Ref, [10]. Copyright 2008 American Chemical Society.

2.2. *Violations of the IPR with EMFs*

Fullerene structures normally conform to the IPR since violations result in higher strain energy. For this reason the five-membered rings should be surrounded by six-membered rings;[28] however, the encapsulation of metals and metal clusters have made possible the synthesis of non-IPR EMFs. The first reports of EMFs with carbon cages containing fused pentagon systems were those of $Sc_2@C_{66}$[115] and $Sc_3N@C_{68}$ (D_3:6140).[110] Other examples are $Sc_2C_2@C_{68}$ (C_{2v}:6073), $Sc_3N@C_{70}$ (C_{2v}:7854), $La_2@C_{72}$ (D_2:10611), $La@C_{72}$, $DySc_2N@C_{76}$ (C_s:17490), $Gd_3N@C_{82}$ (C_s:39663), and $M_3N@C_{84}$ (C_s:51365; M = Gd, Tb, Tm).[75b,104,116–121] On the other hand, spectroscopy along with DFT calculations strongly suggested that the major isomer of $Dy_3N@C_{78}$ and $Tm_3N@C_{78}$ both have the non-IPR carbon cage of symmetry C_2:22010[122] and that $Ce_2@C_{72}$ possesses a non-IPR carbon cage of D_2 symmetry, as in the case of $La_2@C_{72}$.[123] It is interesting to note that as the size of the fullerene increases, the number of fused pentagon systems decreases; for example, $Sc_3N@C_{68}$ (D_3:6140) has three fused pentagon systems while $Gd_3N@C_{82}$ (C_s:39663) and $M_3N@C_{84}$ (C_s:51365) (M = Gd, Tb, Tm) have only one (Figure 5).

Crystallographic data together with theoretical calculations have shown that there is a strong interaction between the encapsulated metal(s) and the fused pentagon system. The electronic donation from the metal or metal cluster is localized mainly in the fused pentagon system, thereby making it more aromatic in character and, therefore, more stable. Akasaka and co-workers have studied the chemical reactivity of $La_2@C_{72}$ and demonstrated that the C–C bonds of the fused pentagon system adjacent to the [5,5] bond hold higher electron density than other C–C bonds of the fullerene cage, while the [5,5] bond itself has the lowest electron density.[40b] Figure 6 shows the HOMO/LUMO distributions

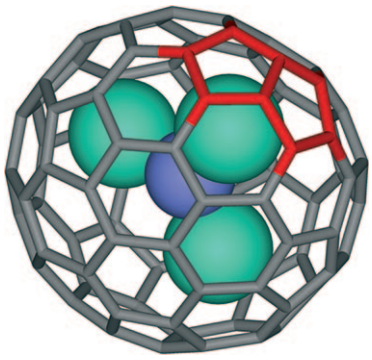

Figure 5. The non-IPR structure of $Gd_3N@C_{84}$ (C_s:51 365). The fused pentagon system is highlighted in red.

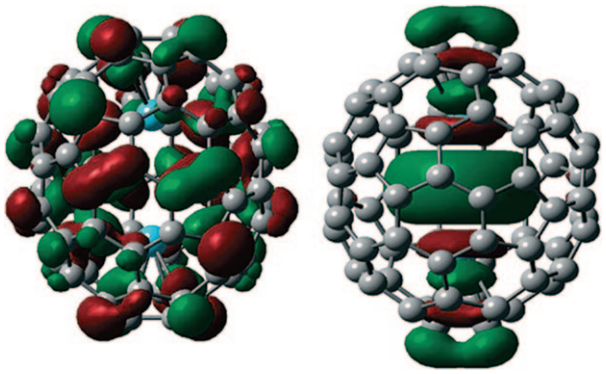

Figure 6. The HOMO (left) and LUMO (right) of $La_2@C_{72}$. Reproduced with permission from Ref. [40b]. Copyright 2008 American Chemical Society.

of $La_2@C_{72}$. It is observed from these orbital distributions that the HOMO is mainly localized on the carbon cage, but it does not contain the two [5,5] bonds corresponding to each fused pentagon system. The LUMO, on the other hand, contains the two La atoms and the two [5,5] bonds. These features of the fused pentagon system can be used to understand the reactivity of non-IPR EMFs, as described by Akasaka and co-workers.[40b,c]

2.3. Purification of EMFs

The separation of isomers and different cage-sized EMFs has traditionally been accomplished by high-performance liquid chromatography (HPLC) using columns specific for fullerenes such as Buckyprep, Buckyprep-M, Buckyclutcher, PBB, and PYE. Linear combinations of these columns, multistep separations, or recycling HPLC chromatography allow the isolation of different EMF isomers.[2–9] Figure 7 shows some common chromatographic stationary phases used in HPLC columns for the separation of EMFs. Although over the years HPLC has been the most powerful technique to separate EMFs, this separation process is usually time consuming and expensive. The main reason for this is that empty cages (such as C_{60} and C_{70}) are usually two orders of magnitude more abundant than EMFs in the extracts of the raw soot. On the other hand, mixtures of isomers usually have

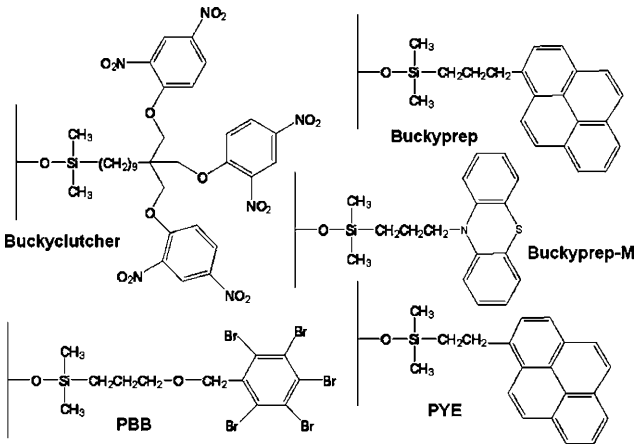

Figure 7. Some common chromatographic stationary phases used in HPLC columns for the separation of EMFs.

very similar retention times, thus requiring longer separation times and consequently it is necessary to use multistep chromatographic separations. Thus, efforts have been made by several research groups to avoid HPLC as much as possible.

2.3.1. Alternative Purification Methods of EMFs

For the aforementioned reasons, approaches other than HPLC to extract and purify EMFs are highly desirable, but only a few are currently available. One of the first methods was the extraction of EMFs from primary soot by using different solvents such as DMF, pyridine, or mixed solvents. Other methods include electrochemical and chemical separations of EMFs from the extracted soot. These methods take advantage of the considerably large HOMO–LUMO gaps of empty fullerenes such as C_{60} and C_{70}. EMFs are more easily oxidized or reduced, then extracted with polar solvents to finally be reduced or oxidized, thereby obtaining neutral EMFs that can be easily separated by HPLC.[66,124]

In 2005, Dorn and co-workers reported the selective isolation of metallic nitride EMFs from other fullerenes obtained during the arcing process.[47a] This method uses a stationary phase composed of a cyclopentadiene-functionalized resin which undergoes Diels–Alder reactions with the fullerenes as they are eluted through the column. Since empty fullerenes and classical EMFs are more reactive than the metallic nitride EMFs, they are retained longer in the column, and thus the metallic nitride EMFs are eluted first. The advantage of this method is that it can separate classical EMFs from metallic nitride EMFs; however, the remaining metallic nitride EMFs are composed of a mixture of isomers and metallic nitride EMFs of different sizes that must be further purified by HPLC. By using this chromatographic method Dorn and co-workers reported the isolation of the I_h isomer of $M_3N@C_{80}$ (M = Sc and Lu) from the isomeric mixture (D_{5h} and I_h).[47b] This was possible because the D_{5h} isomer of $M_3N@C_{80}$ (M = Sc and Lu) is slightly more reactive that its I_h counterpart: all the D_{5h} isomer was removed after three weeks of reaction with the cyclopentadiene-functionalized resin. In principle it is possible to recover the D_{5h} isomer

by a retro-Diels–Alder reaction with maleic anhydride; however, the authors obtained an isomeric mixture of D_{5h} and I_h (that had reacted). Repeating the process several times should finally allow only the D_{5h} isomer to be obtained. The drawback of this method is that it needs several weeks to afford pure samples of the D_{5h} and I_h isomers. Recently, Dorn and co-workers reported another separation method, which also uses a compound that reacts selectively with empty fullerenes through a Diels–Alder reaction and leaves the metallic nitride EMFs unreacted.[47c]

In 2005, Echegoyen and co-workers reported a simple and elegant electrochemical method for the separation of the I_h isomer from the isomeric mixture (D_{5h} and I_h) of $Sc_3N@C_{80}$.[125] The large difference of 270 mV in the first oxidation potential of these two isomers provides a convenient handle to separate the isomers reasonably easily. The selective oxidation of the D_{5h} isomer with a suitable agent leaves the I_h isomer in the neutral state; thus, when the mixture is loaded onto a silica gel column the oxidized isomer is irreversibly adsorbed while the pure I_h isomer is eluted. In the same year Echegoyen and co-workers reported another separation method for the I_h isomer from the isomeric mixture (D_{5h} and I_h) of $Sc_3N@C_{80}$ which involved the selective synthesis of *N*-ethylpyrrolidino-$Sc_3N@C_{80}$.[53,61] Under certain reaction conditions only the I_h isomer reacts, even in the presence of $Sc_3N@C_{78}$. Once the pyrrolidino adduct is isolated it is heated at reflux with maleic anhydride to recover the pure I_h isomer. Stevenson et al. later reported the removal of the D_{5h} isomer by using what they called the "stir and filter approach", again by taking advantage of the higher reactivity of the D_{5h} isomer relative to that of the I_h.[126] The same research group reported in 2007 the selective synthesis of $Sc_3N@C_{80}$ by using plasma additives in the packed rods (the "chemically adjusting plasma temperature, energy, and reactivity"; CAPTEAR method).[127a] Figure 8 shows the results of the CAPTEAR experiments, and illustrates that $Sc_3N@C_{80}$ is obtained exclusively at a given percent of a copper additive. Later, the same research group studied the effect of copper on the yield of metallic nitride EMFs.[127b]

Even though the aforementioned methods offer alternatives to purifying EMFs, there is still a high dependence on HPLC for the isolation these compounds. For classical EMFs, the most important non-HPLC methods focus on maximizing the extraction of fullerenes from the soot by using different solvents and/or by reducing/oxidizing the resulting soot; however, these approaches do not offer reproducible results or good extraction efficiency since the use of HPLC is still needed. In the case of metallic nitride EMFs, efforts have been focused on the separation of the D_{5h} and I_h isomers of $Sc_3N@C_{80}$, which is very difficult by HPLC,[128] but fewer studies have addressed the separation of larger carbon cages or other isomers. There is even a risk that these larger cages are lost during these purification procedures. The chemical separation of metallic nitride EMFs from other fullerenes (empty cages and classical EMFs) by the cyclopentadiene-functionalized resin offers the advantage of yielding a sample of EMFs totally free of empty fullerenes and thus reducing the HPLC separation time. However, it was already reported by Dunsch and Yang that the synthesis of empty cages and other classical EMFs is suppressed by using a reactive gas atmosphere in the arcing process.[7–9] Therefore, additional research on other non-HPLC methods for the purification and isolation of EMFs is still needed.

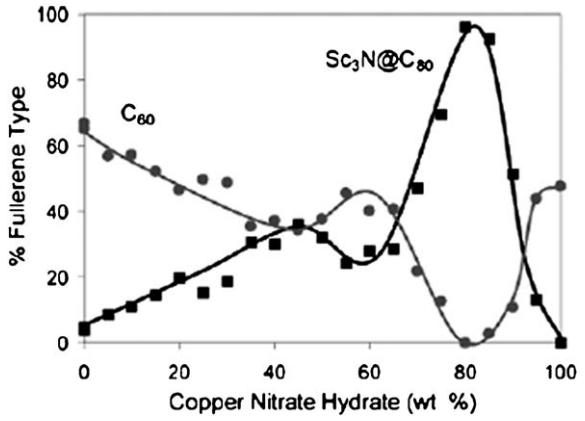

Figure 8. Comparison between the percent of fullerene versus the percent of $Cu(NO_3)_2{\cdot}2.5\,H_2O$ in the CAPTEAR experiment. Reproduced with permission from Ref. [127a]. Copyright 2007 American Chemical Society.

3. Chemical Functionalization of EMFs

In addition to the synthesis and isolation, the chemical functionalization of EMFs has been the main focus of many researchers for two important reasons. First, to improve the characterization of those compounds that could not be isolated or studied by spectroscopy and X-ray crystallography. The second reason is to generate materials that are easy to process for multiple potential applications, such as in optics, molecular electronics, and medicine. In this section we will focus on the different possibilities for the exohedral modification of EMFs, beginning with the first functionalized $La@C_{82}$ derivative reported in 1995 by Akasaka and co-workers.[30a] The different types of functionalization reactions such as Diels–Alder reactions, 1,3-dipolar cycloadditions, Bingel–Hirsch reactions, photochemical reactions, free-radical reactions, and some other addition reactions are reviewed.

Even though all those reactions have given insight into the chemical properties of EMFs, a complete study of the structure–reactivity relationships of EMFs is still lacking. In general, EMFs seem to be quite reactive towards organic functionalization, giving rise to multiple adducts or to a high number of regioisomeric monoadducts. However, a remarkable regioselectivity has been observed in a few cases for both mono- and bisadducts, depending on the nature of the encapsulated metal(s) or metal cluster. The isolation of the obtained isomers is never an easy task—especially in the case of multiadducts—thus making it difficult to study their properties.

A significant number of studies have concerned the I_h isomer of the C_{80} carbon cage. The high symmetry of this carbon cage means that only two possible [1,2] addition sites (that is, involving two adjacent carbon atoms) are available (Figure 9). The double bonds are located at a junction between: 1) a five- and a six-membered ring ([5,6] connec-

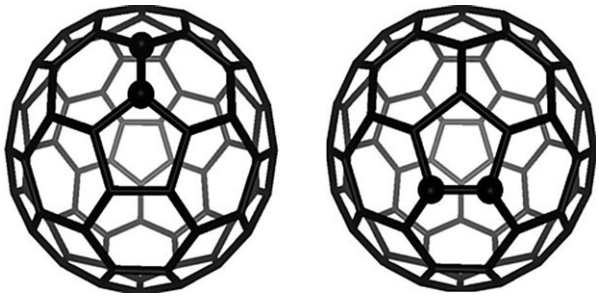

Figure 9. Possible [1,2] addition sites on the I_h-C_{80} cage. Left: The [6,6] ring junction; right: the [5,6] ring junction.

tion) and 2) between two six-membered rings ([6,6] connection). 1,4-Additions (that is, involving two carbon atoms lying opposite in a six-membered ring) have also been reported. Lower symmetry IPR carbon cages have multiple addition sites, either of the [5,6] or [6,6] types, and, therefore, a mixture of several monoadducts that are hard to isolate and characterize is usually obtained after functionalization.

3.1. Photochemical Reactions

3.1.1. Silylation Reaction

In 1995 Akasaka and co-workers reported the first functionalization of an EMF, La@C_{82} (**1a**), with 1,1,2,2-tetrakis(2,4,6-trimethylphenyl)-1,2-disilirane (**2**, Scheme 1). A deaerated solution of **1a** and **2** in toluene was irradiated

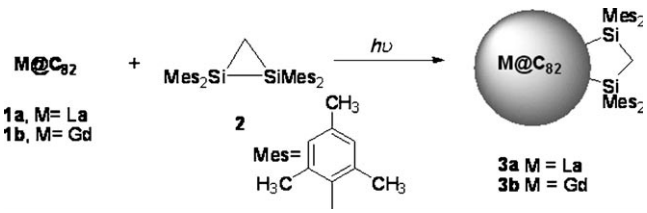

Scheme 1. Photochemical reaction of M@C_{82} (M = La, Gd) with disilirane.

in a sealed tube at 20 °C with a tungsten-halogen lamp to afford a 1:1 mixture of monoadduct isomers **3a**. They were caracterized by FAB MS and EPR spectroscopy.[30] Later, Akasaka and co-workers obtained the analogous compound Gd@C_{82}(Mes_2Si)$_2CH_2$ (**3b**) under the same reaction conditions. Furthermore, the same monoadduct was obtained when **1b** and **2** were heated in toluene at 80 °C for 1 h.[31] To understand why the addition occurred under thermal conditions, while frontier orbital considerations show it is forbidden for C_{82}, C_{60}, and C_{70}, Akasaka et al. studied the photochemical and thermal reactions of **1a** with a derivative of another group IV element, 1,1,2,2-tetrakis(2,6-diethylphenyl)-1,2-digermirane [(Dep_2Ge)$_2CH_2$]. The monoadduct La@C_{82}[(Dep_2Ge)$_2CH_2$] was obtained under both conditions, and characterized by mass spectrometry and EPR spectroscopy. This reactivity has been attributed to the higher electron affinity (stronger electron-accepting characteristics) as well as the lower ionization potential (stronger electron-donating properties) of La@C_{82} compared to empty fullerenes.[32] Thus, the endohedral metal-doping seems to control the exohedral reactivity of the carbon cage. A couple of years later, Akasaka and co-workers presented the bissilylated monoadducts of Pr@C_{82},[33a] Ce@C_{82},[33b] Y@C_{82},[33c] Sc_3N@C_{80},[33c,d] and Ce_2@C_{78}.[33e]

During 2005, Akasaka et al. also studied the chemical reactiviy of the cation and anion of M@C_{82} (M = Y, La, Ce). A solution of M@C_{82} in *ortho*-dichlorobenzene (o-DCB) at room temperature under argon was treated with either a small excess of sodium thiomethoxide (for reduction) or tris(4-bromophenyl)aminium hexachloroantimonate (for oxidation). The photochemical reaction of the M@C_{82} ions with **2** then afforded 1:1 adducts of [M@C_{82}]$^+SbCl_6$. This finding shows the effectiveness of oxidation as a method to increase the reactivity of the M@C_{82}. Interestingly, no product was obtained in the case of the reduced species [M@C_{82}]$^-Na^+$, thus leading to the conclusion that oxidation increases and reduction decreases the reactivity of M@C_{82} in the disilirane photochemical reaction.[34]

3.1.2. Carbene Addition Reactions

In 2004, Akasaka and co-workers reported the regioselective addition of 2-adamantane-2,3-[3*H*]-diazirine (Ad; **4**) to **1a** to form the paramagnetic monoadduct **5** (Scheme 2). Irradiation with a high-pressure mercury lamp of a degassed

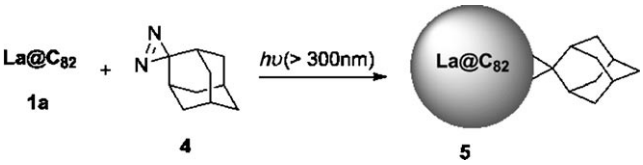

Scheme 2. Carbene addition to La@C_{82}.

solution of **1a** with an excess of **4** in 1,2,4-trichlorobenzene (TCB)/toluene in a sealed tube at room temperature afforded the monoadduct **5**, which was characterized by MALDI-TOF MS, HPLC, EPR spectroscopy, and X-ray crystallography. The crystal structure showed the formation of a fulleroid structure and the positioning of the La atom near the addition site.[35a,b] In 2005, Akasaka, Nagase, and co-workers elucidated the structure of Sc_3C_{82} by ^{13}C NMR spectroscopy and X-ray crystal structure analysis of its derivative functionalized with **4**. The crystallographic analysis showed that it was a metallic carbide EMF, namely Sc_3C_2@C_{80} and not Sc_3C_{82} (the structure proposed by theoretical calculations).[36] In 2007, Akasaka, Nagase, and co-workers used the same carbene addition reaction to characterize the metallic carbide EMF [5,6]-Sc_2C_2@C_{82}(Ad) (C_1).[37] In 2008, two adamentylidene derivatives of La_2@C_{80} (C_s) were also obtained, thus confirming the theoretical prediction that La_2@C_{80} has two electron-rich bonds that could react with **4**.[38] The crystal structure of Gd@C_{82}(Ad) showed the Gd atom to be located at an off-center position near a hexagonal ring along the C_2 axis of the

C_{82} (C_{2v}) cage (in contrast to the anomalous structure proposed earlier).[39] The thermal and photochemical reactions of $La_2@C_{78}$ with **4** gave four and seven isomeric monoadducts, respectively. The addition occurred at both [5,6] and [6,6] bonds around the pole and equator. The X-ray crystal structure of one of the isomers showed an open structure with the two La atoms on the C_3 axis of $La_2@C_{78}$ (D_{3h}).[40a]

Akasaka and co-workers recently reported the reactivity of the non-IPR EMF $La_2@C_{72}$ (D_2:10611), which possesses two fused [5,5] pentagon systems located at the poles of the fullerene. Under photolysis, $La_2@C_{72}$ reacted with **4** to afford six isomeric monoadducts;[40b] longer reaction times afforded at least 15 different bisadducts.[40c] Interestingly, the two addends are located at the fused pentagon regions on each side of the C_{72} cage. Although the largest strain occurs at the [5,5] bonds, these are the least reactive bonds, and the additions occur at the bonds adjacent to these ones. This behavior was ascribed to La stabilization of the [5,5] bonds.[40]

3.1.3. Miscellaneous Reactions

The perfluoroalkylation of $La@C_{82}$ (C_s) was reported by Shinohara and co-workers in 2002 with the purpose of increasing the solubility in highly fluorinated carbon solvents. A degassed and cooled solution of $La@C_{82}$ (C_s) with an excess of perfluorooctyl iodide in toluene was irradiated with a UV lamp over 15 h, and then the $La@C_{82}(C_8F_{17})_2$ was extracted with oxygen-free perfluorohexane. HPLC and mass spectrometric analysis of the product showed the presence of seven different monoadducts and no multiadducts.[41] A benzylation of $Sc_3N@C_{80}$ (I_h) and $Lu_3N@C_{80}$ (I_h) was reported by Dorn, Gibson, and co-workers in 2008, whereby a deoxygenated solution of $M_3N@C_{80}$ (M = Sc, Y) and an excess of benzyl bromide in toluene at room temperature was irradiated at 355 nm for 1 h. The dibenzyl derivatives were isolated by HPLC in 82% and 63% yield (based on their respective unrecovered starting material), respectively. Based on its crystal structure and DFT calculations, it was determined that $Sc_3N@C_{80}(CH_2C_6H_5)_2$ had a 1,4-structure at a [5,6,6] ring junction.[42]

3.2. [4+2] Cycloadditions: Diels–Alder Reactions

The first organic derivative of a metallic nitride EMF was prepared in 2002 by Dorn and co-workers. The single ^{13}C-labeled monoadduct **8** was obtained after heating a solution of $Sc_3N@C_{80}$ **7a** and excess 6,7-dimethoxyisochroman-3-one (99% ^{13}C-labeled; **6**) in TCB at reflux for 24 h (Scheme 3). NMR experiments suggested that the two methylene carbon atoms of **8** were equivalent and the methylene protons non-equivalent, thus indicating a plane of symmetry which bisected the pyrrolidine ring perpendicularly. Therefore, the [4+2] cycloaddition must take place on a localized [5,6] ring junction of the I_h isomer.[43] The crystal structure of the monoadduct **8** was later reported, and showed that the bond between the C–C bond at the [5,6] addition site was elongated and pulled out from the fullerene cage. The Sc_3N cluster was

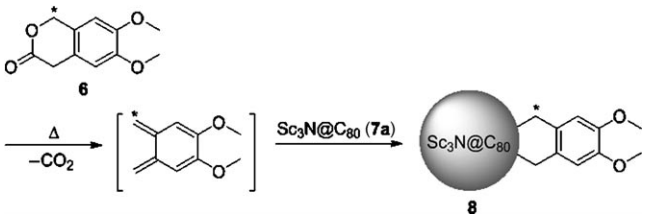

Scheme 3. [4+2] Diels–Alder reaction of $Sc_3N@C_{80}$.

positioned away from the addition site and all the Sc atoms were located close to a [5,6] bond.[44]

In 2005, Stevenson et al. reported the synthesis of some bisadducts of $Gd_3N@C_{80}$[45] by using the same approach used by Dorn and co-workers.[43] Those derivatives were analyzed by HPLC and mass spectrometry, but the regiochemistry of the bisadducts was not described. Also in the same year Akasaka, Nagase, and co-workers[46] reported the reversible and regioselective addition reaction of $La@C_{82}$ (C_{2v}; **1a**) with cyclopentadiene (Cp, **9**), whereby Cp was added in excess to a degassed solution of **1a** in toluene (Scheme 4). The reaction

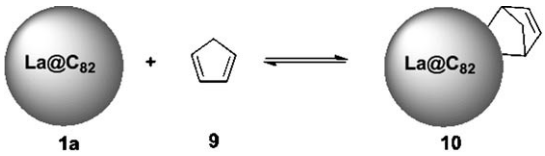

Scheme 4. [4+2] Diels–Alder reaction of $La@C_{82}$ (**1a**) with furan.

was monitored by EPR over two hours in the dark. The single monoadduct **10** was isolated by HPLC in 44% yield. One set of octet signals in the EPR spectrum demonstrated the presence of only one single adduct. Furthermore, the retro-Diels–Alder reaction was obtained at 298 K in toluene, with an activation energy even lower than that of the retro reaction of $C_{60}Cp$.[46] Dorn and co-workers took advantage of the higher reactivity of empty fullerenes and classical EMFs compared to metallic nitride EMFs towards Diels–Alder reactions for the purification of metallic nitride EMFs from the extracted fullerenes.[47a,c] Finally in 2009, Solà and co-workers published a theoretical study of the Diels–Alder reaction of 1,3-butadiene with all the non-equivalent bonds of $Y_3N@C_{78}$. Addition at the [6,6] junction was predicted to form the most stable isomer with the longest bond distance and the largest pyramidalization angle.[48]

3.3. [3+2] Cycloadditions: 1,3 Dipolar Cycloaddition or Prato Reaction

In 2004, Akasaka and co-workers reported the synthesis of a pyrrolidine adduct of $La@C_{82}$ (C_{2v}).[49] A solution of $La@C_{82}$ (C_{2v}) in toluene containing an excess of *N*-methylglycine and paraformaldehyde was heated in a sealed EPR quartz tube at 100 °C for 30 minutes. Three bisadducts and two monoadducts were obtained, and multistep HPLC separation enabled one mono- and one bisadduct to be isolated in pure form. The EPR spectra of the two species

showed the same octuplet hyperfine structure as the starting material. However, the hyperfine coupling constant, *g* value, and peak-to-peak linewidth of the monoadduct were closer to that of the nonderivatized La@C_{82} (C_{2v}) than that of the bisadduct, thus indicating that the monoadduct had a similar electronic structure to that of the parent compound.[49] In the same year, Gu and co-workers studied the same reaction with different M@C_{82} EMFs (M = Gd, Y)[50,51] by using *N*-methylglycine and different aldehydes. Multiple additions were obtained and further isolation of the adducts was not accomplished. Finally, Dorn et al. reported the pyrrolidine derivative of $Sc_3N@C_{80}$ in a patent application, but with few characterization details.[52]

In 2005 Echegoyen and co-workers reported the first pyrrolidine adduct of $Sc_3N@C_{80}$ (I_h)[53] by adding an excess of *N*-ethylglycine and ^{13}C-formaldehyde to a solution of a mixture of $Sc_3N@C_{80}$ (D_{5h}) and (I_h) in *o*-DCB. The mixture was heated for 15 minutes at 120 °C, and a monoadduct **13a** (Scheme 5) was isolated by column chromatography and analyzed with the same techniques used by Dorn and co-

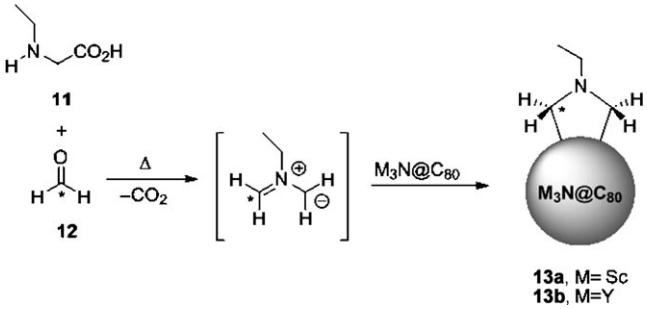

Scheme 5. 1,3-Dipolar cycloaddition of $M_3N@C_{80}$ (I_h; M = Sc, Y).

workers[43] (^{1}H NMR, ^{13}C NMR, and HMQC experiments). This showed that the pyrrolidine ring was formed regioselectively at a [5,6] bond of the $Sc_3N@C_{80}$ (I_h) isomer.[53] The same year, Echegoyen and co-workers reported the first pyrrolidine adduct of $Y_3N@C_{80}$ (I_h, **13b**; Scheme 5), but the cycloaddition occurred at a [6,6] bond for this metallic nitride EMF.[54] Later, Dorn, Gibson, and co-workers reported the functionalization of $M_3N@C_{80}$ (M = Sc, Er) with *N*-methylglycine and ^{13}C-formaldehyde, and they observed a similar addition to a [5,6] bond as observed with the $Sc_3N@C_{80}$ (I_h) isomer.[55]

In 2006, Akasaka and co-workers[56] reported the synthesis and characterization of both [5,6] and [6,6] pyrrolidine derivatives of $La_2@C_{80}$ (**14**; Scheme 6), by using 3-triphenylmethyl-5-oxazolidinone (**15**) as the reagent. The crystal structure as well as the ^{139}La NMR spectrum of the [6,6] adduct showed that the La atoms are fixed, whereas theoretical calculations suggest that the two La atoms can move freely in the case of the [5,6] adduct.[56] Echegoyen and co-workers reported the quantitative thermal isomerization of the [6,6] adduct to the [5,6] adduct of *N*-ethylpyrrolidino-$M_3N@C_{80}$ (M = Y, Er). The [6,6] monoadduct was the kinetic product, and the [5,6] monoadduct the thermodynamic product. Both derivatives were analyzed by NMR spectroscopy and cyclic voltammetry, with the latter technique proving to be excellent for differentiating the two isomers.[58]

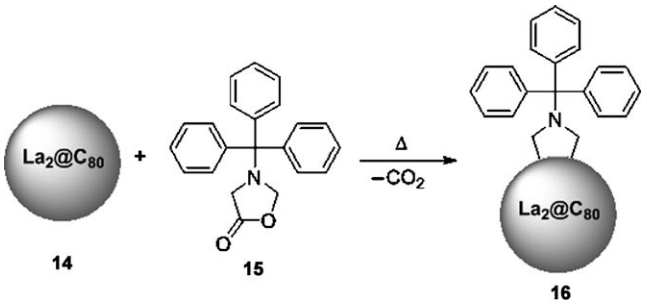

Scheme 6. 1,3-Dipolar cycloaddition of $La_2@C_{80}$.

Poblet and co-workers suggested that the [6,6] adduct is more stable than the [5,6] adduct for metallic nitride EMFs with larger cages and larger charge transfer (Y > Sc).[59] Echegoyen and co-workers reported also the crystal structure of the [5,6]-pyrrolidine monoadduct of $Y_3N@C_{80}$ (**13b**). The N atom was found to be out of the plane of the three Y atoms, and the Y_3N unit presented three different fractional occupancies (0.89, 0.07, and 0.04), thus suggesting that the unit could move inside the cage.[60] Dorn et al. reported the synthesis and thermal isomerization of two monoadducts ([5,6] and [6,6]) of $Sc_3N@C_{80}$ (I_h) and **15**. The [6,6] adduct was thermally converted into the [5,6] adduct.[57] Dorn and co-workers also investigated the 1,3-dipolar cycloaddition reaction of the pure D_{5h} isomer of $Sc_3N@C_{80}$ with **15**, which afforded two monoadducts and two bisadducts. The reactivity of the D_{5h} isomer was higher relative to that of the I_h isomer, and resulted in nine different types of C–C bonds (two symmetric [5,6] bonds, two nonsymmetric [5,6] bonds, three asymmetric [6,6] bonds, and two symmetric [6,6] bonds). NMR spectroscopic analysis suggested that the addition in one of the monoadducts occurred at one of the symmetric [6,6] bonds of the pyracylene unit, whereas in the other monoadduct the addend was predicted to be at a nonsymmetric [6,6] bond.[47b] Later that year, the 1,3-dipolar retrocycloaddition of the *N*-ethylpyrrolidino-$Sc_3N@C_{80}$ (I_h) derivative was reported by Echegoyen and co-workers.[61] The pyrrolidine derivative was heated at reflux in *o*-DCB for 20–24 h in the presence of maleic anhydride, thereby affording 93% of pure $Sc_3N@C_{80}$ (I_h) after column chromatography. The mechanism proposed was the formation of the azomethine ylide on thermal treatment, which could be trapped by the dipolarophile present in the reaction medium.[61]

In 2007, Lu and co-workers studied how the regiochemistry of the 1,3-dipolar reaction with *N*-ethylglycine and formaldehyde is influenced by the size of the cluster in $Sc_xGd_{3-x}N@C_{80}$ ($x = 0$–3).[62] The reaction mixtures were analyzed by HPLC and mass spectrometry and the products were heated again to determine which isomer was the thermodynamic product. Based on the experimental data and theoretical study, it was proved that the [5,6] adduct was favored with the smallest cluster of the series (Sc_3N), whereas the [6,6] adduct was favored in the case of the largest cluster (Gd_3N).[62] A more complete study of the series $Sc_{3-x}Y_xN@C_{80}$ ($x = 0$–3) was later carried out and showed that $Sc_3N@C_{80}$ and $ScY_2N@C_{80}$ formed only [5,6] adducts, whereas $Sc_2YN@C_{80}$ formed both [5,6] and [6,6] adducts. These results suggested

that $Sc_3N@C_{80}$ and $Sc_2YN@C_{80}$ as well as $Y_3N@C_{80}$ and $ScY_2N@C_{80}$ shared nearly the same electronic structure and frontier orbitals.[63] Dorn, Balch et al. prepared the [6,6]-*N*-tritylpyrrolidino derivatives of the ellipsoidal $Sc_3N@C_{78}$ [D_{3h}-(78:5)] in which the internal trimetallic cluster (Sc_3N) was planar. The solution of $Sc_3N@C_{78}$ [D_{3h}(78:5)] and **15** in chlorobenzene was refluxed for 3 h, and then purified by HPLC to give two mono- and one bisadduct. The two monoadducts were characterized by NMR spectroscopy, mass spectrometry, and DFT calculations, and one of them was analyzed by X-ray diffraction. It was found that the Sc_3N moiety remained in the horizontal plane of the D_{3h}(78:5) cage, far away from the site of addition.[64]

Finally, Echegoyen and co-workers reported new pyrrolidine derivatives of metallic nitride EMFs with different dyad substituents (phthalocyanine (Pc), and ferrocene) attached to the pyrrolidine ring.[65] A [5,6] adduct was obtained for $Sc_3N@C_{80}$ (I_h) and a [6,6] adduct was obtained for $Y_3N@C_{80}$ (I_h).[65]

3.4. [2+1] Cycloadditions: Bingel–Hirsch Reaction

In 2003, Alford and co-workers reported the first water-soluble $Gd@C_{60}$ derivative.[66] By using the Bingel reaction, an insoluble polymeric material from the $Gd@C_{60}$ fraction was treated with diethyl bromomalonate (**17a**) in the presence of an alkali metal hydride and tetrahydrofuran as the solvent. The addition of up to 10 malonate groups was detected by mass spectrometry. This ester derivative was then hydrolyzed to the water-soluble carboxylic acid derivative $Gd@C_{60}(C(CO_2H)_2)_{10}$.[66] A couple of years later Diener et al. used the same approach to modify the α-emitting radionuclides $^{212}Pb@C_{60}$ into a soluble derivative.[67] In 2005, Akasaka, Nagase, and co-workers synthesized the singly bonded EPR-inactive monoadduct $La@C_{82}CBr(CO_2C_2H_5)_2$ and characterized it by NMR spectroscopy and X-ray crystallography.[68] It was assumed, on the basis of theoretical calculations, that the nucleophilic reaction took place in the first step, followed by the oxidation of the intermediate.[68] In later studies, Akasaka and co-workers reported that five monoadducts were obtained when the reaction was conducted at room temperature;[69] four of them were EPR-inactive, thus suggesting the formation of singly bonded adducts and cycloadducts. When the reaction temperature was increased to 60 °C, the reaction proceeded much faster and yielded the bisadduct with C_{2v} symmetry as the major product, which was characterized by X-ray crystallography and electrochemistry as well as EPR and UV/Vis spectroscopy. The same bisadduct can be obtained by using NaH instead of DBU as the base.[69] In 2005, Echegoyen and co-workers reported the first monomethanofullerene derivative **18a** of the I_h isomer of $Y_3N@C_{80}$ by cyclopropanation with **17a** and 1,8-diazobicyclo-[5.4.0]undec-7-ene (DBU; Scheme 7) that occurred selectively at a [6,6] double bond.[54] The $Er_3N@C_{80}C(CO_2C_2H_5)_2$ monoadduct **18b** (Scheme 7) was also prepared and characterized by HPLC and mass spectrometry. Voltammetric data suggested it was most likely a [6,6] regioisomer.[58] An extensive study of these derivatives later concluded that the

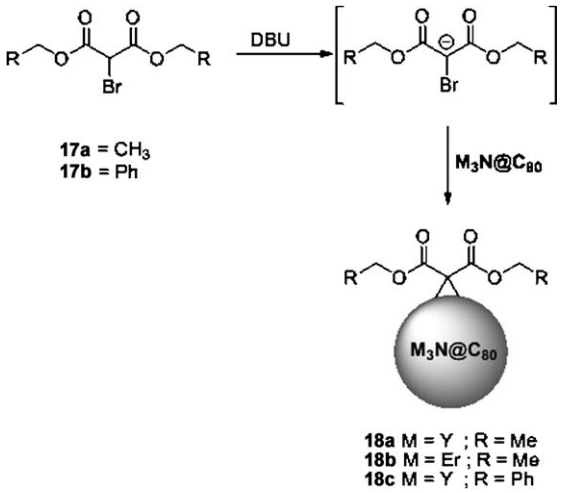

Scheme 7. Cyclopropanation of $M_3N@C_{80}$ (M = Y, Er).

[6,6] regioisomer has a very high stability, since no retro-cycloaddition of **18a** took place (in contrast to C_{60}).[70] The methanofullerene **18c** synthesized with $Y_3N@C_{80}$ was identified by X-ray diffraction as a fulleroid in which the addition bond is broken (see C1–C9 in Figure 10). The [6,6] bond of the addition site is indeed open and, in contrast to the crystal structure of the methanopyrrolidino **13b** derivative, one metal ion points directly towards the open bond.[71] This open ring could explain the higher stability of this [6,6] isomer.[58]

In 2008, Echegoyen and co-workers studied for the first time the reactivity of larger Gd_3N-EMFs (C_{80}, C_{84}, and C_{88}) towards the cyclopropanation reaction by using **17a** and DBU.[72] For the C_{80} cage, a monoadduct and a bisadduct were isolated after a very short reaction time at room temperature. In the case of the C_{84} cage, a monoadduct was formed after 20 minutes under identical reaction conditions. No addition to the C_{88} cage was detected even after an increase in the temperature to 60 °C. This trend in the reactivity—$C_{80} > C_{84} > C_{88}$—was explained in terms of the degree of pyramidalization at the C atom, with C_{80} having the highest degree of pyramidalization and C_{88} the lowest.[72]

Mono- and bisadducts of bis(ethoxycarbonyl)methano derivatives of $Sc_3N@C_{78}$ (D_{3h}) were recently reported by Dorn, Gibson, and co-workers.[73] Two Bingel adducts of $Y_3N@C_{80}$ with anthraquinone and Pc moieties were synthesized and characterized by Echegoyen and co-workers.[65]

3.5. Free-Radical Reactions

In 1995, Suzuki, Kato et al.[74] described the diphenylmethano-$La@C_{82}$ adducts, which where synthesized by the addition of excess diphenyldiazomethane to a solution of $La@C_{82}$ in toluene in an EPR tube. The reaction was followed by EPR spectroscopy at 60 °C over 3.7 h, without any significant change in the hyperfine coupling constants being observed. Mass spectrometric analyses revealed the addition of up to three addends, but no characterization of these adducts was reported.[74] In 2005, Yoza and co-workers presented the crystal structure of one of the three isomers

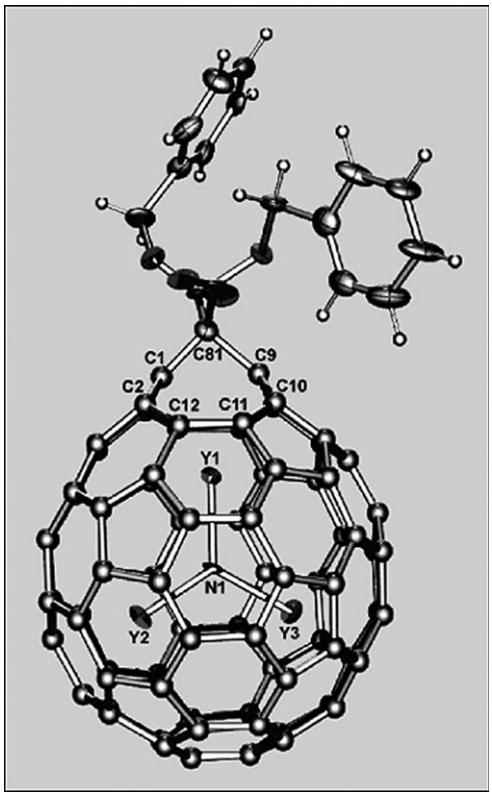

Figure 10. Structure of the Bingel adduct **18c** (thermal ellipsoids at 50%). Reproduced with permission from Ref. [71]. Copyright 2007 American Chemical Society.

of the $La@C_{74}(C_6H_3Cl_2)$ adducts isolated from the extraction of the soot with TCB.[75] According to theoretical calculations, the radical present on the C_{74} (D_{3h}) cage can be trapped with dichlorophenyl radicals produced during the extraction. Similar adducts were observed for the non-IPR compound $La@C_{72}$.[75] Kareev, Boltalina et al. published the isolation and characterization (MS and ^{19}F NMR) of two diamagnetic stable isomers of $Y@C_{82}(CF_3)_5$. These were obtained by reaction of a $Y@C_{82}$-enriched extract with $AgCF_3CO_2$ in a quartz reactor under dynamic vacuum at 400 °C for 10 h.[76] Later in 2008, Akasaka, Nagase, and co-workers published the synthesis, isolation, and full characterization of four isomers of $La@C_{82}(CH_2C_6H_5)$, which were obtained by reaction of **1a** with 3-triphenylmethyl-5-oxazolidine.[77] Theoretical calculations suggested that the addition sites were kinetically controlled.[77]

In 2007 Stevenson, Botalina, and co-workers reported the synthesis, isolation, and characterization (^{19}F NMR, MS, and electrochemistry) of fluoroalkylated derivatives of $Sc_3N@C_{80}$ (D_{5h} and I_h). In this approach, CF_3I gas was used as the fluroalkylating agent at high temperature.[78] Dorn, Gibson, and co-workers reported the first methano-$Sc_3N@C_{80}$ derivatives by using a free-radical reaction.[79] The hydrogen atom from the labeled methylene group was abstracted by $Mn(OAc)_3{\cdot}2H_2O$, which was followed by addition up to eight times to the EMF cage. The products were characterized by NMR and UV/Vis spectroscopy, as well as mass spectrometry. Calculations suggested that these derivatives were [6,6] adducts, similar to the diphenyl malonate adduct of $Y_3N@C_{80}$ described earlier.[71] Ten malonate groups were added to $Lu_3N@C_{80}$ under similar reaction conditions.[79]

3.6. Other Reactions

3.6.1. Miscellaneous Reactions

A gas-phase derivatization of M-EMFs (M = Nd, Ce) with vinyl acetate was carried out by Liu and co-workers in 1997 using an electron impact (EI) mass spectrometer.[80] The formation of the electrophile $C_2H_3O^+$ (m/z 43) in the gas phase and its subsequent addition to the carbon cage were proposed.[80] The m/z signals corresponding to $M@C_{80}$ and $M@C_{82}$ (M = Nd, Ce) were observed together with other signals with higher m/z values (+43).

In 2002, Gu and co-workers reported the addition of diazocompounds ($N_2{=}C(CO_2Me)(R)$, R = phenyl or naphthyl) to $Tb@C_{82}$ in the presence of the copper(I) catalyst $[(Cu(MeCN)_4]PF_6$. MALDI-TOF MS and FTIR spectroscopy suggested that up to six $C(CO_2Me)(R)$ groups were added to the carbon cage. Unfortunately, no further characterization or separation of the multiadducts was achieved.[81a] Later in 2004, Gu and co-workers reported the [2+2] cycloaddition of $Gd@C_{82}$ with anthranilic acid in the presence of isoamylnitrite. Two monoadducts in a ratio of 8:1 were isolated by HPLC and characterized by mass spectrometry and electrochemistry.[81b]

In 2007, Yang and co-workers reported the synthesis of a $Dy@C_{82}$ derivative bearing a single phosphorus substituent by a regio- and chemoselective reaction of $Dy@C_{82}$ with dimethyl acetylenedicarboxylate and triphenylphosphine. This derivative was characterized by X-ray crystallography.[82]

3.6.2. Hydroxylation Reactions

In 1997, Pei and co-workers prepared the first water-soluble endohedral metallofullerenols of $Gd@C_{2n}$. They refluxed a toluene extract of gadolinium EMF in the presence of potassium metal under N_2 for 2 h, and then hydrolyzed the dry precipitate with water. This mixture of compounds was analyzed by LD-TOF MS and FTIR spectroscopy, as well as by X-ray photoelectron spectroscopy (XPS), which predicted an average of 20 hydroxy groups per cage.[83] Then in 1999, Wilson et al. reported the water-soluble EMFs $^{165}Ho@C_{82}(OH)_x$ ($x = 24$–26), which were obtained under alkaline phase-transfer conditions. These derivatives were neutron-activated to ^{166}Ho to study their use as potential radioactive tracers.[84] During the same year, the water-soluble endohedral metallofullerenol $Pr@C_{82}O_m(OH)_x$ ($m \approx 10$ and $x \approx 10$) was prepared from pure $Pr@C_{82}$ and concentrated nitric acid, followed by hydrolysis. This metallofullerenol was characterized by FTIR spectroscopy, XPS, and LD-TOF MS.[85]

Shinohara and co-workers used a phase-transfer reaction to obtain the metallofullerenols $M@C_{82}(OH)_x$ (M = Gd, La, Ce, Dy, Er).[86] Dorn and co-workers synthesized $Sc_3N@C_{80}O_m(OH)_x$ ($m \approx 10$ and $x \approx 10$) by treatment of $Sc_3N@C_{80}$ with sodium metal and subsequent hydrolysis in

the presence of air.[87] Gu and co-workers studied the nucleophilic addition of glycine esters to $Gd@C_{82}$, where the presence of hydroxy groups arising from the excess of NaOH competed with them for addition to the cage, thereby forming $Gd@C_{82}(NHCH_2CO_2R)_m(OH)_x$ (R = Me, $m = 1$–4, $x = 0,1$ or R = Et, $m = 1$–8, $x = 0,1$).[88] Tang and co-workers prepared $Gd@C_{82}(OH)_2$ by treating a solution of $Gd@C_{82}$ in toluene with 30% hydrogen peroxide over 7 h without oxygen.[89] Dorn and co-workers also used hydrogen peroxide to obtain hydroxylated derivatives of $Gd_3N@C_{80}$.[90c] Wang and co-workers reported the water-soluble EMF $Gd@C_{82}O_6(NHCH_2CO_2H)_8(OH)_{16}$, which was synthesized by the reaction of $Gd@C_{82}O$ with an excess of an alkaline solution of β-alanine.[90a,b] Later, Wang, Feng, and co-workers reported the preparation of metallofullerenols $Sc_pGd_{3-p}N@C_{80}O_m(OH)_x$ ($p = 1,2$; $m \approx 12$; $x \approx 26$) by using sodium metal followed by hydrolysis.[90d]

Tremendous progress has been made in the last few years in understanding the reactivity of EMFs. Nevertheless, there is still no clear understanding of the exact effect that the metal cluster exerts on the chemical properties of the carbon cage. We can only infer from the examples discussed that there is a synergistic relationship between the cage and the metal species when it comes to reactivity. We have shown examples where the exohedral reactivity is dictated by the nature of the metal and others where the cage symmetry, size, and shape dictate the position of the metals, the reactivity, and the availability of addition sites.

4. Electrochemistry of EMFs

Electrochemical methods provide valuable information about the interaction between the entrapped species and the carbon cages in these special supramolecular structures. Fortunately, the high sensitivity of these methods is well adapted to the microgram quantities in which these materials are sometimes available. When coupled to EPR spectroscopy, electrochemistry also allows the determination of the electronic properties (for example,the HOMO and LUMO localization) of the entrapped moieties and the cage. In many cases, electrochemistry has also proved itself as a faster and cheaper alternative to the conventional chromatographic methods for purification.

4.1. Electrochemistry/EPR of Classical EMFs

The influence of the encapsulated metal as well as the size and symmetry of the carbon cage on the electrochemical behavior of the classical EMFs is now well documented, thanks to the systematic report of the electrochemistry of the $M@C_{82}$, $Yb@C_{2n}$, and $Ca@C_{2n}$ compounds.

4.1.1. The $M@C_{82}$ Family: Influence of the Metal

Different electrochemical behavior of the $M@C_{82}$ compounds has been reported by the research groups of Suzuki, Akasaka, Gu, Dunsch, and Wang (Table 1).[33a,129–131]

Table 1: Redox potential (in V versus Fc^+/Fc) of the $M@C_{82}$ compounds. The round brackets denote the cage isomer.

Fullerene	$E\,ox_2$	$E_{1/2}\,ox_1$	$E_{1/2}\,red_1$	$E_{1/2}\,red_2$	$E_{1/2}\,red_3$	$E_{1/2}\,red_4$	$E_{1/2}\,red_5$	$E_{1/2}\,red_6$
$La@C_{82}$ (C_{2v})[129h]	1.07	0.07	−0.42	−1.37	−1.53	−2.26	−2.46	
$La@C_{82}$ (C_s)[33a]	1.08	−0.07	−0.47	−1.40	−2.01	−2.40		
$Pr@C_{82}$ (C_{2v})[33a]	1.08	0.07	−0.39	−1.35	−1.46	−2.21		
$Pr@C_{82}$ (C_s)[33a]	1.05	−0.07	−0.48	−1.39	−1.99	−1.99		
$Ce@C_{82}$ (C_{2v})[129h]	1.08	0.08	−0.41	−1.41	−1.53	−1.79	−2.25	−2.50
$Gd@C_{82}$ (C_{2v})[129h]	1.08	0.09	−0.39	−1.38	−2.22			
$Y@C_{82}$ (C_{2v})[129h]	1.07	0.10	−0.37	−1.34	−2.22	−2.47		
$Sm@C_{82}$ (C_{2v})[129l]			−0.28	−0.63	−1.52	−1.88	−2.03	−2.32
$Yb@C_{82}$ (C_s)[130]			−0.33	−0.65	−1.58	−1.81		
$Yb@C_{82}$ (C_2)[130]			−0.60	−0.76	−1.33	−1.73		
$Yb@C_{82}$ (C_{2v})[130]			−0.33	−0.67	−1.56	−1.90		
$Ca@C_{82}$ (C_2)[131]			−0.59	−0.74	−1.30	−1.70		
$Ca@C_{82}$ (II)[131]			−0.65	−0.96	−1.55	−1.90		
C_{82} (C_2)[132]			−0.47	−0.80	−1.42	−1.84		

A group of compounds—$Ce@C_{82}$, $Gd@C_{82}$, $Y@C_{82}$, and the major (C_{2v}) and minor (C_s) isomers of $La@C_{82}$ and $Pr@C_{82}$—were characterized by a very low electrochemical potential gap ($\Delta E_{gap} = E\,ox_1 - E\,red_1 < 0.50$ V). The very easy and reversible first oxidation step (close to that of the ferrocene/ferrocenium couple) and the six reversible reduction steps means that these compounds are very good electron donors and electron acceptors. This is significantly different behavior from that observed for the empty cage C_{82} (Table 1). EPR studies showed that $Y@C_{82}$[129d] and both isomers of $La@C_{82}$[129c,133] are radical species, and ^{13}C NMR studies[33b,134] showed that the electrochemically generated monoanions of these compounds are diamagnetic. Therefore, their low electrochemical gap is probably a consequence of an open-shell electronic structure. All of these experimental observations have been rationalized by assuming that the metal transfers three electrons to the cage ($M^{3+}@C_{82}^{3-}$). A good linear relationship was found between the first reduction and first oxidation potentials and the ionic radius of the metal (r_M^{3+}).[129h] It was assumed that the metal ion is not in the center of the cage, and that the SOMO of the compound has its largest electron density on the section of the cage that is closer to the metal ion. The smaller the metal, the closer to the cage it can be, and therefore the tighter the electrons of the SOMO are bound.

In contrast to this electrochemical behavior, no oxidation step could be observed for $Sm@C_{82}$ and all the isolated isomers of $Ca@C_{82}$, $Yb@C_{82}$, and $Tm@C_{82}$, thus indicating a much larger electrochemical gap. It was assumed from the diamagnetism that the metal adopts a +2 formal oxidation

state in these compounds, thereby leading to a $M^{2+}@C_{82}^{2-}$ electronic structure.

From these studies, we can conclude that the formal oxidation state of the entrapped metal and its size have a clear influence on the redox properties of the EMFs.

4.1.2. The Yb@C_{2n} and Ca@C_{2n} Families: Influence of the Cage Structure

The electrochemistry of EMFs is also highly dependent on the structure of the carbon cage, as observed by Gu and co-workers when studying the Yb@C_{2n}[130] and Ca@C_{2n}[131] families (Table 2). No anodic signal was observed for any of these compounds, which make them large band-gap compounds. Their redox behavior was interpreted assuming a +2 formal oxidation state for the Yb or Ca atoms and, therefore, a closed-shell electronic configuration. A very striking observation is the dramatic difference in the electron-accepting abilities of isomers of the same endohedral fullerene. This difference reached 0.22 V for the isomers of Yb@C_{76} and even 0.3 V between two isomers of Yb@C_{82}. The cage size also influenced the reduction potentials. The C_s and C_{2v} isomers of Yb@C_{82} were the best electron acceptors of the family, while isomer II of Yb@C_{76} was the worst. In general, however, these EMFs were better electron acceptors than the corresponding empty cages. EMFs with bigger cages, Yb@C_{82} and Yb@C_{84}, also accepted a fifth electron more easily than the others.

Table 2: Half-wave redox potential (in V versus Fc^+/Fc) of the M@C_{82} compounds.

Fullerene	$E_{1/2}$red$_1$	$E_{1/2}$red$_2$	$E_{1/2}$red$_3$	$E_{1/2}$red$_4$
Yb@C_{74} (II)[130]	−0.52	−0.96	−1.55	−1.99
Yb@C_{76} (I)[130]	−0.46	−0.83	−1.46	−1.89
Yb@C_{76} (II)[130]	−0.68	−1.02	−1.59	−2.01
Yb@C_{78}[130]	−0.48	−0.79	−1.46	−1.83
Yb@C_{80}[130]	−0.57	−0.95	−1.55	−1.90
Yb@C_{82} (C_s)[130]	−0.33	−0.65	−1.58	−1.81
Yb@C_{82} (C_2)[130]	−0.60	−0.76	−1.33	−1.73
Yb@C_{82} (C_{2v})[130]	−0.33	−0.67	−1.56	−1.90
Yb@C_{84} (II)[130]	−0.63	−0.88	−1.26	−1.64
Yb@C_{84} (III)[130]	−0.49	−0.68	−1.57	−1.79
Yb@C_{84} (IV)[130]	−0.46	−0.72	−1.34	−1.54
Ca@C_{76}[131]	−0.61	−0.99	−1.57	−1.97
Ca@C_{82} (C_2)[131]	−0.65	−0.96	−1.55	−1.90
Ca@C_{82} (II)[131]	−0.59	−0.74	−1.30	−1.70
Ca@C_{84} (II)[131]	−0.64	−0.90	−1.27	−1.65

4.1.3. Endohedral Dimetallofullerenes

The electrochemical behavior of M_2 moieties encapsulated in C_{72}, C_{80}, and C_{82} cages have also been reported[33c,40b,133c,135] (Table 3) and compared to that of the monometallic-EMFs. The similarities in the redox properties of the dimetallic moieties La_2 and Ce_2 encapsulated in the non-IPR C_{72} cage[40b,135b] suggested that they share a very similar electronic structure. The same applies to La_2 and Ce_2 encapsulated in a C_{80} cage, as well as to Sc_2 and Er_2 entrapped in a C_{82} cage. Since a higher degree of charge transfer between the encapsulated moiety and the cage is believed to occur in these structures (six electrons), it was expected that these compounds would be less prone to reduction. However, it was observed that the electron-accepting ability was better than anticipated. In particular, La_2@C_{80} and Ce_2@C_{80} were even easier to reduce than La@C_{82} and Ce@C_{82}. This finding is probably a result of the LUMO being localized on the dimetal cluster, as predicted by calculations on La_2@C_{80}. In contrast, the electron-donating ability of La_2@C_{80} and Ce_2@C_{80} was significantly weaker.

Table 3: Redox potentials (in V versus Fc^+/Fc) of M_2@C_{2n} compounds; comparison with La@C_{82} and Ce@C_{82}.

Compound	Eox$_2$	Eox$_1$	Ered$_1$	Ered$_2$	Ered$_3$
La_2@C_{72} (D_2)[40b]	0.75	0.24	−0.68	−1.92	
Ce_2@C_{72} (D_2)[135e]	0.82	0.18	−0.81	−1.86	
La_2@C_{78} (D_{3h})[135c]	0.62	0.26	−0.40	−1.84	−2.28
La_2@C_{80} (I_h)[133c]	0.95	0.56	−0.31	−1.72	−2.13
Ce_2@C_{80} (I_h)[135d]	0.95	0.57	−0.39	−1.71	
Sc_2@C_{82} (I)[135a]	0.10	−0.12	−1.26	−1.88	
Sc_2@C_{82} (III)[135a]		0.07	−0.87	−1.29	−1.85

4.1.4. Influence of Exohedral Derivatization

There is considerable interest in the scientific community to clarify how the reactivity of the endohedral fullerenes is influenced by their structure, as well as how the electronic properties of the endohedral fullerenes are modified upon derivatization. Once again, electrochemical methods have helped considerably in this area. Several derivatives of M@C_{82} have been prepared and their electrochemical behavior recorded (Table 4).[34,35a,68,69b,77,81b,136]

Table 4: Maximum potentials (in V versus Fc+/Fc) of M@C_{82} and some derivatives (differential pulse voltammetry).

Compound	Eox$_2$	Eox$_1$	Ered$_1$	Ered$_2$	Ered$_3$
La@C_{82} [C_{2v}][129h]	1.07	0.07	−0.42	−1.37	−1.53
La@C_{82}-adamentylidene[35a]	1.01	−0.01	−0.49	−1.44	−1.79
La@C_{82}-$(Mes_2Si)_2CH_2$I[136]		−0.07	−0.50	−1.71	−1.75
La@C_{82}-$[CH(COOC_2H_5)_2]_2$[69b]		0.08	−0.32	−1.57	
La@C_{82}-$CBr(COOC_2H_5)_2$[68]	0.85	0.38	−0.66	−1.31	−1.47
La@C_{82}-benzyl [a][77]		0.25	−0.68	−1.02	−1.21
La@C_{82}-benzyl [b][77]		0.21	−0.95	−1.40	
La@C_{82}-Benzyle [c][77]		0.17	−0.84	−1.42	−1.74
La@C_{82}-benzyl [d][77]		0.15	−1.05	−1.15	−1.81
La@C_{82}-$CHClC_6H_3Cl_2$ [b][77]		0.24	−0.91	−1.39	
La@C_{82}-$CHClC_6H_3Cl_2$ [d][77]		0.25	−0.98	−1.07	−1.34
Gd@C_{82} (C_{2v})[129i]	1.08	0.20	−0.25	−1.25	
Gd@C_{82}-C_6H_4 (I)[81b]		0.26	−0.97		
Gd@C_{82}-C_6H_4 (II)[81b]		0.38	−0.55		
Y@C_{82} (C_{2v})[129h]	1.07	0.10	−0.37	−1.34	−2.22
Y@C_{82}-$(Mes_2Si)_2CH_2$I (I)[136]	0.10	−0.10	−0.55	−1.36	
Y@C_{82}-$(Mes_2Si)_2CH_2$I(II)[136]		−0.03	−0.42		

$La@C_{82}$ was found to be very reactive towards disilirane or diazo compounds (because of its high electron-accepting ability) and towards benzyl radicals (because of its open-shell configuration). Akasaka and co-workers reported that $La@C_{82}$-adamentylidene and $La@C_{82}$-$(Mes_2Si)_2CH_2I$ showed lower electron-accepting ability, but a higher electron-donating ability than the parent $La@C_{82}$ (see Table 4). This behavior was ascribed to electron donation from the exohedral addend to the fullerene. However, these derivatives were—similar to the parent $La@C_{82}$—still EPR-active. The behavior of the singly bonded adducts $La@C_{82}$-$CBr(COOC_2H_5)_2$, $La@C_{82}$-benzyl, and $La@C_{82}$-$CHClC_6H_3Cl_2$ was very different, since these compounds were found to be more difficult both to oxidize and to reduce, and showed, therefore, a much larger electrochemical gap than $La@C_{82}$. The EPR specra showed that the derivatization reactions forced $La@C_{82}$ to acquire a closed-shell electronic configuration. In contrast, the bisadduct $La@C_{82}$-$[CH(COOC_2H_5)_2]_2$ was again EPR active and a low-band-gap compound. The disilane derivatives of $Y@C_{82}$ showed a behavior very similar to that of the disilane derivative of $La@C_{82}$, whereas the benzyne derivatives of $Gd@C_{2n}$ were characterized by a much larger electrochemical band gap. Unfortunately, no information about EPR activity was given in this case.

Besides the $M@C_{82}$ compounds, a few other derivatives of classical EMFs have been prepared and studied by electrochemistry, such as the adamantylidene derivatives of $M_2@C_{2n}$ ($M = La$, Ce and $n = 36$, 39, 40; Table 5).[40,137] These results confirmed the electron-donating nature of the adamantylidene group towards the endohedral fullerene, since each addition of an adamantylidene group systematically shifted the first oxidation and first reduction towards more cathodic potentials. Interestingly, the magnitude of the shift was dependent on the position of the addend on the carbon cage, as nicely illustrated by the La_2C_{78}-adamentylidene monoadduct family,[40a] and by the number of addends.[40c] Therefore, the electrochemical properties of EMFs can be finely tuned by adding one or more electron-donating groups.

The main conclusion that can be drawn from the studies of classical EMFs is that their electrochemical behavior is usually very different from that of the empty cages. This is mainly due to charge transfer between the entrapped metal or cluster and the cage; the nature and extent of the charge transfer depends on the properties of the metals. Nevertheless, EMFs with the same entrapped metals can also show dramatic differences in their reductive or oxidative behavior as a result of differences in their electronic structure. Exohedral derivatization can also alter the electrochemical behavior of EMFs, particularly in the case of electron-donating groups. Therefore, EMFs show a very large range of redox properties: some of them can be very easily oxidized and reduced—such as the historically important $La@C_{82}$—whereas others are difficult to oxidize—such as $Ca@C_{82}$.

These dramatic differences have been exploited in the efficient purification of large quantities of endohedral fullerenes by using either one or a combination of chemical and electrochemical oxidative or reductive reactions. The first report of such an interesting purification method was published in 1998 by Diener and Alford, who described the separation of the empty cages from gadolinium endohedral fullerenes (which have a small band gap) in the arcing soot by using an electrochemical reduction followed by a selective chemical reoxidation.[124g] The procedure was later improved to obtain three different fractions of $Gd@C_{2n}$ compounds easily and quickly.[124d] This is a fast, efficient, and economic alternative to the standard purification method used in this field, namely HPLC.

Table 5: Half-cell potentials (in V versus Fc^+/Fc) of $La_2@C_{72}$ and $La_2@C_{78}$ and some adamantylidiene derivatives.

Compound	$E ox_2$	$E ox_1$	$E red_1$	$E red_2$
$La_2@C_{72}$ (D_2)[40b]	0.75	0.24	−0.68	−1.92
$La_2@C_{72}$-adamentylidene[40c]	0.67	0.15	−0.76	−2.00
$La_2@C_{72}$-(adamentylidene)$_2$[40c]	0.57	0.02	−0.86	−2.08
$La_2@C_{78}$ (D_{3h})[135c]	0.62	0.26	−0.40	−1.84
$La_2@C_{78}$-adamentylidene (M_1)[40a]	0.63	0.23	−0.43	−1.82
$La_2@C_{78}$-adamentylidene (M_2)[40a]	0.69	0.16	−0.46	−1.83
$La_2@C_{78}$-adamentylidene (M_3)[40a]	0.61	0.21	−0.48	−1.83
$La_2@C_{78}$-adamentylidene (M_4)[40a]	0.63	0.13	−0.44	−1.78
$La_2@C_{80}$ (I_h)[133c]	0.95	0.56	−0.31	−1.72
$La_2@C_{80}$-adamentylidene[137]	0.86	0.49	−0.36	−1.78
$Ce_2@C_{80}$(I_h)[135d]	0.95	0.57	−0.39	−1.71
$Ce_2@C_{80}$-adamentylidene[137]	0.89	0.47	−0.43	

4.2. Electrochemistry/EPR of Nonclassical EMFs: Metallic Nitride and Metallic Carbide Fullerenes

Electrochemistry has played a crucial role in establishing the interesting electronic properties of nonclassical metallic nitride fullerenes. Most of the studies have concerned the abundant $Sc_3N@C_{80}$[33c,58,125,128,138] and other metallic nitride clusters entrapped in the I_h-C_{80} cage. However, there has been increasing interest during the last two years in compounds with larger cages, such as C_{84}, C_{88}, C_{92}, and C_{96}, which can now be prepared in reasonable amounts with many lanthanide metals, such as Gd, Nd, Pr, Ce, and La.[9]

4.2.1. The $M_3N@C_{80}$ Family: Influence of the Metal

HPLC purification of the soot extract obtained upon arcing graphite rods packed with Sc_2O_3 yields mainly a mixture of two isomers of $Sc_3N@C_{80}$: the predominant I_h isomer and the less abundant D_{5h} isomer. The first electrochemical studies were first carried out on the mixture of isomers (Figure 11). The anodic scan of the cyclovoltammogram showed the superposition of the signals of both isomers. Interestingly, the D_{5h} isomer was much easier to oxidize than the icosahedral one (by 270 mV), thereby confirming that the redox properties of endohedral fullerenes depend dramatically on the symmetry of the carbon cages. Echegoyen and coworkers exploited this large difference in the oxidation potentials of the two isomers to separate them.[125] By choosing a chemical oxidant (tris(*p*-bromophenyl)aminium hexachloroantimonate, "magic blue") with a redox potential

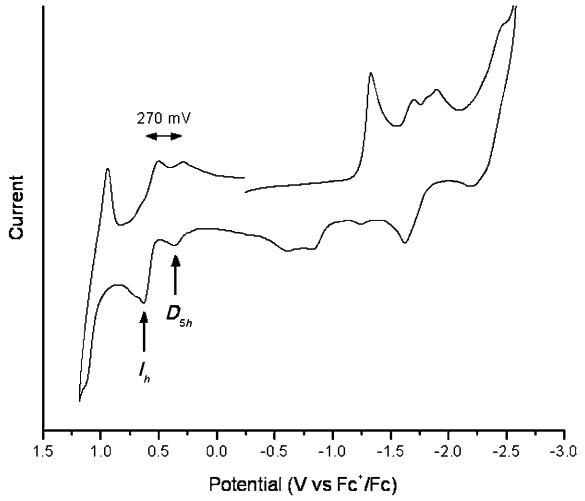

Figure 11. Cyclic voltammogram of the isomeric mixture (I_h and D_{5h}) of $Sc_3N@C_{80}$ obtained in *o*-DCB + 0.05 M $(n\text{Bu})_4\text{NPF}_6$ (scan rate 100 mV s^{-1}).

intermediate between those of the two isomers, the D_{5h} isomer was preferentially oxidized and removed from the mixture by simple filtration over SiO_2. The electrochemistry of the pure icosahedral isomer of $Sc_3N@C_{80}$ was then reported.[125] This isomer oxidizes in two distinct steps, the first one being reversible even at low scan rates (0.1 V s^{-1}). Despite the high negative charge on the cage (−6), $Sc_3N@C_{80}$ could be reduced in at least three irreversible steps in *o*-DCB. These reduction steps became reversible when scanning at faster scan rates, which suggests that a chemical step followed the electronic transfer (EC mechanism). (Recently, it was also shown that reversibility can be attained by changing the solvent to a mixture of acetonitrile and toluene.[138b]) The nature of the chemical step remains unclear. Complete electrolysis of $Sc_3N@C_{80}$ at a potential corresponding to the first reduction, followed by reoxidation at 0 V yielded the starting material. The radical anion was generated either by chemical reduction with sodium/potassium alloy or by one-electron electrolysis. The EPR spectrum[125,139] consisted of 22 lines, assigned to 3 equivalent scandium nuclei with a large hyperfine splitting of 55.6 G. This finding suggested that the C_3 symmetry of the endohedral cluster was conserved in the radical anion. The authors suggested that a pyramidalization of the flat Sc_3N cluster may occur upon reduction. Recently, Popov and Dunsch found using DFT calculations that the C_{3v} conformer is the ground state of $[Sc_3N@C_{80}]^{\cdot-}$, and that cluster rotation is considerably hindered.[112b]

Interestingly, all the $M_3N@C_{80}$ (I_h) compounds studied so far in *o*-DCB showed an electrochemical behavior quite similar to that of $Sc_3N@C_{80}$, with irreversible reduction steps and reversible oxidation processes (Table 6).[58,114,138a,140] However, the nature of the metal has a notable influence on the reduction potentials and a less-marked influence on the oxidation potentials (see Table 6). The case of $Sc_3N@C_{80}$ seems unique, since this compound has a significantly lower electrochemical gap than the others. The EPR spectrum of the $Sc_3N@C_{80}$ radical anion,[139] together with quantum calculations suggested a major contribution of the cluster to the LUMO.[112b,142] For the other metallic nitride EMFs, it is now believed that there is no significant contribution from the cluster to either the LUMO or the HOMO.[112b,143] To rationalize the influence of the metal on the electrochemical behavior of these compounds, it was therefore assumed that the significant charge transfer between the cluster and the cage depends on the electronic properties and size of the metals. The effective metal valences (Table 6) were determined by high-energy spectroscopic studies of some of these compounds, and showed that scandium, the smallest and most electronegative metal of the series, seemed to transfer less electron density to the cage than thulium or dysprosium.[141] This explains why $Sc_3N@C_{80}$ is the easiest to reduce. In contrast, the weaker electron acceptors $Gd_3N@C_{80}$, $Nd_3N@C_{80}$, and $Pr_3N@C_{80}$ are made from the largest and least electronegative metals of the family. Interestingly, $Sc_3N@C_{80}$ was also the easiest compound to reduce and the lowest band-gap compound of the D_{5h} isomers (see the last four entries in Table 6).[138a]

Table 6: Relevant redox potential (in V versus Fc$^+$/Fc), metal electronegativities (χ), and effective valencies of the $M_3N@C_{80}$ compounds obtained in *o*-DCB + 0.05 M $(n\text{Bu})_4\text{NPF}_6$.

Compound	χ	Effective valency	$Ep_c\,red_1$[a]	$Ep_c\,red_2$[a]	$E_{1/2}\,ox_1$[a]	ΔE_{gap}[a]
$Sc_3N@C_{80}$ (I_h)[58]	1.36	2.4[141a]	−1.29	−1.56	0.59	1.88
$Sc_3N@C_{80}$ (I_h)[128]	1.36	2.4[141a]	−1.24	−1.62	0.62	1.86
$Sc_3N@C_{80}$ (I_h)[33c]	1.36	2.4[141a]	−1.22	−1.59	0.62	1.84
$Sc_3N@C_{80}$ (I_h)[33c]	1.36	2.4[141a]	−1.27		0.57	1.84
$Lu_3N@C_{80}$ (I_h)[138a]	1.27		−1.40		0.64	2.04
$Tm_3N@C_{80}$ (I_h)[140d]	1.25	2.9[141b]	−1.43	−1.78	0.65	2.08
$Er_3N@C_{80}$ (I_h)[58]	1.24		−1.42	−1.80	0.63	2.05
$Y_3N@C_{80}$ (I_h)[58]	1.22		−1.41	−1.83	0.64	2.05
$Dy_3N@C_{80}$ (I_h)[140a]	1.22	2.8[141c]	−1.37	−1.86	0.70	2.07
$Gd_3N@C_{80}$ (I_h)[140c]	1.20		−1.44	−1.86	0.58	2.02
$Nd_3N@C_{80}$ (I_h)[114b]	1.14		−1.42	−1.89	0.63	2.05
$Pr_3N@C_{80}$ (I_h)[114b]	1.13		−1.41	−1.84	0.59	
$ScYErN@C_{80}$ (I_h)[140b]			−1.55	−1.97	0.64	
$Sc_3N@C_{80}$ (D_{5h})[138a]	1.36		−1.33		0.34	1.67
$Lu_3N@C_{80}$ (D_{5h})[138a]	1.27		−1.41		0.45	1.86
$Tm_3N@C_{80}$ (D_{5h})[140d]	1.25		−1.45		0.39	1.84
$Dy_3N@C_{80}$ (D_{5h})[140a]	1.22		−1.40	−1.85	0.40	1.80

[a] E_{pc} denotes the cathodic peak potential and $E_{1/2}$ half-wave potential. $\Delta E_{gap} = E_{1/2}\,ox_1 - E_{pc}\,red_1$.

4.2.2. *The $Gd_3N@C_{2n}$, $Nd_3N@C_{2n}$, $Pr_3N@C_{2n}$, $Ce_3N@C_{2n}$, and $La_3N@C_{2n}$ Families: Influence of the Cage*

A dramatic influence of the cage structure was unveiled by Echegoyen and co-workers when studying the electro-

chemistry of the $Gd_3N@C_{2n}$ family, with cages ranging from C_{80} to C_{88} (Figure 12 and Table 7).[9,140c]

$Gd_3N@C_{86}$ and the two non-IPR metallic nitride EMFs $Gd_3N@C_{82}$ (C_s:39663)[116] and $Gd_3N@C_{84}$ (C_s:51365)[118] showed three irreversible reduction and one reversible oxidation processes, a behavior qualitatively similar to that of the IPR $Gd_3N@C_{80}$ (I_h). In contrast, both reductions and oxidations are reversible for $Gd_3N@C_{88}$. Remarkably, changing the cage size does not affect significantly the reduction potential of these compounds, which displayed very similar first reduction potentials (Table 7), but dramatically influenced their oxidation ability. These results strongly suggest that the HOMO of the metallic nitride EMFs are probably cage-centered. A significant lowering of the electrochemical band gap was observed when increasing the cage size from C_{80} to C_{88}. Similar observations regarding the reversibility of the redox steps and the electrochemical band gap (Table 7) were made in the case of the $Nd_3N@C_{2n}$ and $Pr_3N@C_{2n}$ families.[114]

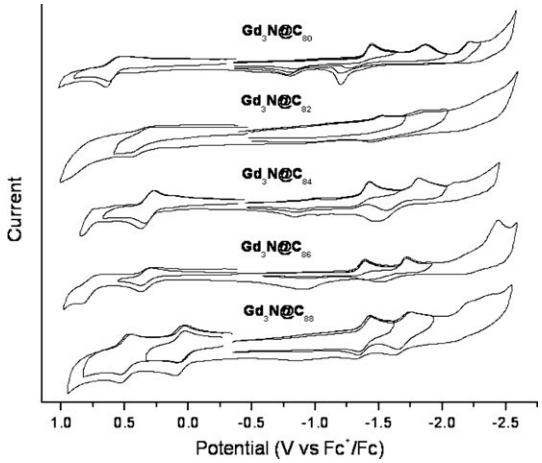

Figure 12. Cyclic voltammograms of $Gd_3N@C_{2n}$ ($40 \leq n \leq 44$) compounds obtained in *o*-DCB + 0.05 M $(n\text{Bu})_4\text{NPF}_6$ (scan rate 0.1 V s^{-1}).

The redox behavior of $Gd_3N@C_{88}$—that is, the reversibility in both oxidation and reduction and the very low HOMO–LUMO gap—was later found to be characteristic of all of the metallic nitride clusters encapsulated in a C_{88} cage (Nd, Pr, and Ce were examined).[9,114] In contrast to the $M_3N@C_{80}$ family, this $M_3N@C_{88}$ family displayed few differences in their oxidation and reduction potentials. This was presumably due to the very similar electronic properties of Gd, Nd, Pr, and Ce (including their electronegativity) and a negligible contribution of the cluster to both the HOMO and LUMO.[64] It was very surprising that such low-band-gap fullerenes were the most abundant species in the soluble extract of the arcing soot in the case of Nd, Pr, and Ce. Only $La_3N@C_{88}$ showed a different behavior, with irreversible reduction steps and a slightly larger electrochemical band gap. This is probably an indication of a different symmetry for this carbon cage, although this has not been firmly established yet.[113]

Interestingly, the very recently reported $M_3N@C_{92}$[143] and $M_3N@C_{96}$[113,143] (M = Pr, Ce, and La) again showed irreversible reductive behavior and a significantly larger electrochemical band gap than the $M_3N@C_{88}$ compounds (Table 7). Three reduction steps and one or two reversible oxidation steps were observed for these compounds (Table 8).

Table 7: Redox potentials (in V versus Fc^+/Fc) of the $M_3N@C_{2n}$ compounds obtained in *o*-DCB + 0.05 M $(n\text{Bu})_4\text{NPF}_6$.

Compound	$Ep_c\,red_1$	$Ep_c\,red_2$	$E_{1/2}\,ox_1$	$E_{1/2}\,ox_2$	ΔE_{gap}[a]
$Gd_3N@C_{80}$ (I_h)[140c]	−1.44	−1.86	0.58		2.02
$Gd_3N@C_{82}$[9]	−1.53	−1.87	0.38		1.91
$Gd_3N@C_{84}$ (C_s)[9]	−1.37	−1.76	0.32		1.69
$Gd_3N@C_{86}$[9]	−1.39	−1.72	0.33		1.72
$Gd_3N@C_{88}$[9,140c]	−1.43	−1.74	0.06	0.49	1.49
$Nd_3N@C_{80}$ (I_h)[114b]	−1.42	−1.90	0.63		2.05
$Nd_3N@C_{84}$[114b]	−1.44	−2.02	0.31		1.75
$Nd_3N@C_{86}$[114b]	−1.46	−1.79	0.36		1.82
$Nd_3N@C_{88}$[114]	−1.36	−1.75	0.07	0.53	1.43
$Pr_3N@C_{80}$ (I_h)[114b]	−1.41	−1.81	0.59		2.00
$Pr_3N@C_{86}$[114b]	−1.48	−1.80	0.31		1.79
$Pr_3N@C_{88}$[114b]	−1.34	−1.72	0.09	0.54	1.43
$Pr_3N@C_{92}$[143]	−1.46		0.35		1.81
$Pr_3N@C_{96}$[143]	−1.51	−1.86	0.14	0.53	1.65
$Ce_3N@C_{88}$[114b]	−1.30	−1.57	0.08	0.63	1.38
$Ce_3N@C_{92}$[143]	−1.48		0.32		1.81
$Ce_3N@C_{96}$[143]	−1.50	−1.84	0.18	0.67	1.68
$La_3N@C_{88}$[114b]	−1.36	−1.67	0.21	0.66	1.57
$La_3N@C_{92}$[143]	−1.44	−1.64	0.36		1.80
$La_3N@C_{96}$[143]	−1.54	−1.77	0.14	0.53	1.68

[a] $\Delta E_{gap} = E_{1/2}\,ox_1 - E_{pc}\,red_1$.

Table 8: Cathodic peak potentials and anodic half-wave potentials (in V versus Fc^+/Fc) of $Sc_3N@C_{68}$, $Sc_3N@C_{78}$, and $Dy_3N@C_{78}$, in comparison with $M_3N@C_{80}$.

Compound	$Ep_c\,red_1$	$Ep_c\,red_2$	$E_{1/2}\,ox_1$	$E_{1/2}\,ox_2$	ΔE_{gap}[a]
$Sc_3N@C_{80}$ (I_h)[128]	−1.24	−1.62	0.62		1.86
$Sc_3N@C_{68}$ (D_3)[144]	−1.45	−2.05	0.33	0.85	1.88
$Sc_3N@C_{78}$[73]	−1.54		0.12		1.66
$Dy_3N@C_{80}$ (I_h)[140a]	−1.37	−1.86	0.70		2.07
$Dy_3N@C_{78}$[140a]	−1.54	−1.93	0.47		2.01

[a] $\Delta E_{gap} = E_{1/2}\,ox_1 - E_{pc}\,red_1$.

The electrochemical properties and EPR spectra of some trimetallic nitride EMFs with cages smaller than C_{80} were also reported (Table 8).[73,140a,144] It was expected that $Sc_3N@C_{68}$, which possesses a non-IPR cage of D_3 symmetry,[115,145] would show a very different behavior than the IPR $Sc_3N@C_{80}$ (I_h), because of their very different cage structures. Dunsch and co-workers observed two irreversible reduction steps for $Sc_3N@C_{68}$[144] that were cathodically shifted compared to those of $Sc_3N@C_{80}$ (Table 8). The main difference between the two compounds was observed in the oxidative scan: The donating ability of $Sc_3N@C_{68}$ was found to be significantly larger than that of $Sc_3N@C_{80}$ (I_h). The radical cation[144] $[Sc_3N@C_{68}]^{+}$ and radical anion[146] $[Sc_3N@C_{68}]^{-}$ were generated by electrolysis and both characterized by EPR spectros-

copy. The EPR spectra consisted of 22 lines, which indicated three equivalent scandium atoms, with a small hyperfine splitting of 1.28 G for the cation and 1.75 G for the anion. Based on the smaller hyperfine splitting, compared to that of $[Sc_3N@C_{80}]^{-\bullet}$,[139] a main delocalization of the unpaired spin on the cage was proposed. This delocalization confirmed the contribution of the cage to the HOMO of these compounds. Dunsch and co-workers also reported the redox behavior of $Dy_3N@C_{78}$,[140a] and very recently Dorn and co-workers reported that of $Sc_3N@C_{78}$.[73] These EMFs showed two irreversible reduction steps and one reversible oxidation step. Their electron-accepting ability was also significantly weaker and their electron-donating ability stronger than that of the parent metallic nitride EMF with an I_h-C_{80} cage.

Since the metallic nitride cluster is believed to transfer six electrons to the cage in these EMFs, Poblet and co-workers proposed that the energy difference between the LUMO + 3 and LUMO + 4 of the empty fullerene should be a good estimation of the HOMO–LUMO gap of the endohedral fullerene.[111,147] These energy differences were computed, and an excellent correlation was found between them and the experimentally measured electrochemical band gaps.[143] This finding confirmed the ionic model of metallic nitride EMFs and highlighted the dependency of the electrochemical properties of metallic nitride EMFs on the topology of the different cages.

4.2.3. *Influence of Exohedral Derivatization*

The electrochemistry of [1,2] cycloaddition adducts of metallic nitride endohedral fullerenes with a C_{80}-I_h cage has been reported.[58] Interestingly, the electrochemical behavior of the monoadducts depends dramatically on the location of the addend, either at a [6,6] or [5,6] site. [5,6] Adducts exhibit reversible cathodic electrochemical properties, while [6,6] adducts exhibit irreversible behavior. So far, electrochemistry has been used as a tool to determine the position where the functionalization has occurred. The best illustration is probably the pyrrolidine adducts of $Er_3N@C_{80}$ reported by Echegoyen and co-workers.[58] The [6,6] derivative exhibited very similar behavior to that of the nonderivatized $Er_3N@C_{80}$, with two irreversible reduction waves. Two oxidation waves could be observed on the anodic side, the first irreversible and the second reversible. While the second wave is similar to the first oxidation wave of the nonderivatized $Er_3N@C_{80}$, the first oxidation was addend-based and led to the removal of the addend from the carbon sphere.[148] The [5,6] derivative exhibited very similar anodic behavior, but showed a contrasting cathodic behavior with three reversible reduction waves. Remarkably the [5,6]-pyrrolidino-$Sc_3N@C_{80}$ and the [5,6] Diels–Alder derivative of $Sc_3N@C_{80}$ exhibited a behavior similar to that of [5,6]-pyrrolidino-$Er_3N@C_{80}$, whereas the [6,6]-pyrrolidino-$Y_3N@C_{80}$ and the [6,6] open methanofullerene derivatives of $Er_3N@C_{80}$, $Y_3N@C_{80}$, and $Gd_3N@C_{80}$ exhibited an electrochemical behavior similar to that of [6,6]-pyrrolidino-$Er_3N@C_{80}$ (Table 9).

The electrochemical properties of a bisadduct was reported in the case of $Gd_3N@C_{80}$,[72] and compared to that of the pristine metallic nitride EMF and the monoadduct (Figure 13). A Bingel–Hirsch reaction was performed, and two methano groups were added on the cage, presumably at two [5,6] ring junctions. Despite the possibility of the formation of several regioisomers, only one was isolated and its purity confirmed by multistep HPLC. The cyclic voltammogram of the isolated bisadduct showed two clearly identifiable irreversible reductive steps and one reversible oxidative step. Interestingly, the addition of one and two methano groups to $Gd_3N@C_{80}$ did not systematically shift the reduction potentials cathodically, as reported for C_{60} derivatives and for the adamantylidene adducts of $La@C_{82}$. The redox potential of the nonderivatized $Gd_3N@C_{80}$ and of the mono- and bisadducts were surprisingly similar (Table 9) to

Table 9: Redox potentials (in V versus Fc^+/Fc) of some [1,2] cycloadducts of $Er_3N@C_{80}$, $Sc_3N@C_{80}$, $Y_3N@C_{80}$, and $Gd_3N@C_{80}$.

Compound	$Ep\,red_1$	$Ep\,red_2$	$E_{1/2}\,ox$[a]	Reduction behavior at 0.1 $V s^{-1}$
$Er_3N@C_{80}$ (I_h)[58]	−1.42	−1.80	0.63	irreversible
[5,6]-pyrrolidino-$Er_3N@C_{80}$[58]			0.64	reversible
[6,6]-pyrrolidino-$Er_3N@C_{80}$[58]			0.64	irreversible
[6,6]-methano-$Er_3N@C_{80}$[58]			0.60	irreversible
$Sc_3N@C_{80}$ (I_h)[55]	−1.29	−1.56	0.59	irreversible
[5,6]-pyrrolidino-$Sc_3N@C_{80}$[58]	−1.18	−1.57	0.62	reversible
[5,6]-Diels–Alder-$Sc_3N@C_{80}$[58]	−1.16	−1.54	0.62	reversible
$Y_3N@C_{80}$ (I_h)[55]	−1.41	−1.83	0.64	irreversible
[6,6]-pyrrolidino-$Y_3N@C_{80}$[58]			0.65	irreversible
[5,6]-pyrrolidino-$Y_3N@C_{80}$[58]	−1.30	−1.65		reversible at 20 $V s^{-1}$
$Gd_3N@C_{80}$ (I_h)[140c]	−1.44	−1.86	0.58	irreversible
$Gd_3N@C_{80}$-$[C(CO_2Et)_2]$[72]	−1.39	−1.83	0.58	irreversible
$Gd_3N@C_{80}$-$[C(CO_2Et)_2]_2$[72]	−1.40	−1.88	0.59	irreversible
$Gd_3N@C_{84}$ (C_s)[140c]	−1.37	−1.76	0.32	irreversible
$Gd_3N@C_{84}$-$[C(CO_2Et)_2]$[72]	−1.43	−1.77	0.28	irreversible

[a] Based on the endohedral cage.

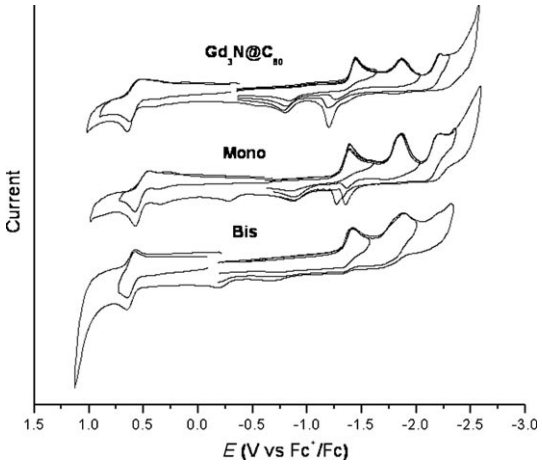

Figure 13. Cyclic voltammograms of a) I_h-$Gd_3N@C_{80}$, b) [6,6]-$Gd_3N@C_{80}$-$C(CO_2Et)_2$, and c) $Gd_3N@C_{80}$-$[C(CO_2Et)_2]_2$ in NBu_4PF_6/*o*-DCB with ferrocene as the internal standard; 100 $mV s^{-1}$ scan rate. Reproduced from Ref. [72]. Copyright The Royal Society of Chemistry.

that of the non-IPR $Gd_3N@C_{84}$ and its methano adduct. Two irreversible reduction steps and one reversible oxidation were also observed for $Gd_3N@C_{84}$-$[C(CO_2Et)_2]$.[72]

The [1,4] adducts obtained by photochemical bissilylation[33d] and radical trifluoromethylation[78] of $Sc_3N@C_{80}$ also showed reversible reductive behavior (Table 10). The oxidation of $Sc_3N@C_{80}$-$(Mes_2Si)_2CH_2$ led to the removal of the addend from the carbon cage, as in the case of pyrrolidino adducts of C_{60} and $Sc_3N@C_{80}$.[148] Interestingly, the redox potentials of these compounds directly reflected the electronic properties of the addend. The highly electron accepting fluorine atoms shifted the first oxidation and first reduction towards more anodic potentials, whereas the electron-donating silicon atoms shifted the first reduction potential to more negative potentials.

Table 10: Redox potentials (in V versus Fc^+/Fc) of some [1,4] derivatives of $Sc_3N@C_{80}$.

Compound	Ep red$_1$	$E_{1/2}$ ox[a]	$E_{1/2}$ ox[b]	Reduction behavior at 0.1 V s^{-1}
$Sc_3N@C_{80}$ (I_h)[58]	−1.29		0.59	irreversible
$Sc_3N@C_{80}$-$(Mes_2Si)_2CH_2$[33d]	−1.45	0.08		reversible
$Sc_3N@C_{80}$-$(CF_3)_2$[78]	−1.16		0.47	reversible

[a] Based on one addend. [b] Based on the endohedral cage.

Very recently the first electrochemical study of donor–acceptor dyads with $Sc_3N@C_{80}$ or $Y_3N@C_{80}$ as acceptors was reported by Echegoyen and co-workers.[21,65] The chosen electron donors were extended tetrathialfulvalene (exTTF) and ferrocene (Fc). The exTTF adduct of $Y_3N@C_{80}$ was very unstable and was rapidly oxidized to an anthraquinone (AQ) adduct. The voltammograms obtained usually showed a superposition of the signals of the endohedral fullerene and the electroactive addends. Once again, the shape of the endohedral-based reduction events was indicative of the position of the addend on the carbon cage. The reversible reductive behavior observed in the case of $Sc_3N@C_{80}$ confirmed that a [5,6]-ferrocenyl pyrrolidine adduct was synthetized, whereas the irreversibility obtained in the case of $Y_3N@C_{80}$ showed that a [6,6] adduct was formed. The ferrocenyl pyrrolidine based oxidations were found to be irreversible, a probable consequence of the electrochemical retrocycloaddition.[148] The redox potentials measured for these compounds are reported in Table 11.

Results for the metallic nitride EMFs confirmed that the electrochemical behavior of these compounds is somewhat influenced by the entrapped moiety, which is believed to formally transfer six electrons to the cage. The large number of metallic nitride EMFs synthesized with cages ranging from C_{68} to C_{96} also allowed the dependency of the redox behavior on the cage topologies to be rationalized for the first time. Finally, it was also established that the redox behavior of the exohedrally derivatized endohedral metallofullerenes depends dramatically on the position of the addend on the carbon cage.

Table 11: Redox potentials (in V versus Fc^+/Fc) of donor–acceptor dyads (acceptors: $Y_3N@C_{80}$ and $Sc_3N@C_{80}$; donors: exTTF, Fc) and comparison with donor model compounds.

Compound	Eox$_3$	Eox$_2$[a]	Eox$_1$[b]	Ered$_1$	Ered$_2$	Ered$_3$
$Y_3N@C_{80}$-exTTF[65]	0.90		0.23	−1.28	− 1.77	−2.22
$Y_3N@C_{80}$-AQ[65]		0.67		−1.34	−1.72	
$Y_3N@C_{80}$-Fc[65]	0.66	0.57	0.07	−1.41	−1.77	
$Sc_3N@C_{80}$-Fc[21]	1.09	0.61	0.15	−1.14	−1.53	−2.25
exTTF-CHO[65]			0.06			
AQ-CH_2OH[65]				−1.50	−1.84	
Fc-CHO[65]			0.20			

[a] Based on the endohedral cage. [b] Based on one addend.

The metallic nitride EMFs are not the only nonclassical EMFs studied by electrochemistry: the electrochemistry of some metallic carbide endohedral fullerenes was also reported (Table 12). Some similarities were observed between the voltammograms of $Sc_2C_2@C_{82}$ and $Er_2@C_{82}$ and that of isomer III of $Sc_2@C_{82}$.[135a] These similarities are now well understood by assuming that these species have the same C_{82} cage. The electronic structure of this metallic carbide endohedral fullerene was established by DFT calculations[37] to be $(Sc_2C_2)^{4+}C_{82}^{4-}$. $Sc_3C_2@C_{80}$ is paramagnetic and, thus, has a very small electrochemical band gap in *o*-DCB.[149] The charge state of this compound was established by DFT calculations to be $(Sc^{3+})_3C_2^{3-}C_{80}^{6-}$.[102] Interestingly the redox state of the molecule does not seem to influence the formal oxidation state of the Sc atoms or the charge on the cage, but directly affects the formal charge on the C_2 moiety. Therefore, the C_2 moiety displayed a remarkable flexibility in terms of charge, and could be varied sequentially from +2 (first oxidation) to −3 (third reduction).

Table 12: Relevant redox potentials (in V versus Fc^+/Fc) of metallic carbide fullerenes.

Fullerene	Eox$_1$	Ered$_1$	Ered$_2$	Ered$_3$
$Sc_2C_2@C_{82}$ (III)[135a]	0.16	−0.95	−1.38	
$Sc_3C_2@C_{80}$ (I_h)[149]	−0.06	−0.50	−1.64	−1.82
$Sc_2@C_{82}$ (III)[135a]	0.07	−0.87	−1.29	−1.85
$Er_2@C_{82}$[135a]	0.19	−0.87	−1.26	

5. Potential Applications of EMFs

The rich electronic properties of the endohedral fullerenes offer very promising applications. The previous section showed that the HOMO–LUMO gap of these materials is highly dependent on the nature of the entrapped moiety, the size and symmetry of the cage, and on exohedral derivatization. Therefore, the band gap can be finely tuned, which is a clear asset for potential applications in molecular electronics. On the other hand, the relative inertness of the carbon cage could lead to medical applications for some

EMFs with highly paramagnetic or radioactive entrapped species. We report here the most recent advances in the potential use of EMFs in electric or electrooptical devices and in medicine.

5.1. EMFs for Molecular Electronics and Photonics

Aside from the large range of HOMO–LUMO gaps exhibited by these compounds, some show very interesting electronic and electrooptical properties. However, only a few reports on the full incorporation of endohedral metallofullerenes in nanoelectronic devices have so far been published.

Fullerenes, in particular higher order ones (C_{70} and above), usually show large nonlinear optical (NLO) responses, because of their highly polarizable π-electron cloud. Charge transfer between the encapsulated moiety and the cage in metallofullerenes leads to an even larger π-electron density on the cage, and these compounds are therefore expected to show even better NLO properties. These properties have been either measured or calculated with DFT for some metallofullerenes.[150] The encapsulation of one metal seems to result in the effective enhancement of NLO properties of fullerenes such as C_{74}[150c] and C_{82}.[150b,d] However, the size of the metal encapsulated is an important factor, and large metals, such as La, are preferable to smaller ones such as Sc.[150e] Interestingly—and quite unfortunately—the encapsulation of a second metal atom leads to a weaker NLO response than that of the empty cage.[150d]

Yang et al. showed that the photocurrent efficiency of a device based on a poly(3-hexylthiophene) film can be enhanced by doping with Dy@C_{82}.[20] This effect was attributed to a facile photoinduced electron transfer between the film and the EMF. In a ferrocene adduct of $Sc_3N@C_{80}$ (I_h), recently reported by Echegoyen and co-workers,[21] photoinduced electron transfer between the ferrocene moiety and the fullerene was detected, and the radical ion pair obtained was significantly stabilized relative to a similar ferrocene–C_{60} dyad. The application of metallofullerenes to the field of photovoltaics thus seems even more promising than that of the more conventional fullerenes.

Some films of EMFs were shown to have semiconductive properties, depending on the number of functional groups on the carbon cage and the temperature, as demonstrated recently with the Gd@$C_{82}(OH)_x$ compounds.[22] The n-type field effect transistor behavior of thin films of $La_2@C_{80}$ has been known since 2003,[151a] and some very recent calculations suggest that it may function as a single-molecule transistor.[151b] Several factors influencing the efficiency of an electromagnetic-based nanotransistor were predicted, such as the nature and geometry of the endohedral–metal cluster and the total charge present in the system.

These properties can be further modified by incorporation of EMFs into carbon nanotubes to form so-called "peapods". In these, the EMFs modulate the band gap of the nanotubes, and both classical[23–25] and nonclassical[6,7,26] metallofullerenes have been inserted in carbon nanotubes. In the case of Gd@C_{82}, a combination of elastic strain and charge transfer between the metallofullerene and the nanotube led to a modulation of the band gap by up to 0.5 eV. Field-effet transistors based on Gd@C_{82} peapods showed an ambipolar behavior with both p- and n-type characteristics.[23] This interesting behavior is a direct consequence of the unique properties of Gd@C_{82}, since it was not observed in the case of C_{60} peapods.

5.2. Application of EMFs in Medicine

The advantages of using endohedral metallofullerenes as contrast agents in magnetic resonance imaging (MRI) are now well recognized.[8,14] Their ability to reduce the spin relaxation time of water protons (quantified by their substantially relaxivity factor R_1) is better than that of the currently used Gd^{III} chelates (Table 13 and Figure 14).[152] Furthermore, their surface can be derivatized as much as needed, and the presence of the carbon cage prevents the release of toxic Gd in organisms. Most of the studies involve classical EMFs, such as derivatives of Gd@C_{2n},[14–16,18,19,86b,90a,b,153] but recent reports also concern nonclassical EMFs, such as derivatives of $Gd_3N@C_{2n}$.[90c,d]

Table 13: Relaxivities R_1 of some classical and nonclassical endohedral Gd fullerenes and comparison with a Gd chelate complex currently used as an MRI contrast agent (DTPA = diethylenetriaminepentaacetic acid; the magnetic field used is given in brackets).

Compound	R_1 [$mM^{-1}s^{-1}$]
Gd@C_{60}-$(OH)_x$[19,153]	83.2–97.7 (1.4 T)
Gd@C_{60}-$[C(COOH)_2]_{10}$[19]	15–24 (1.4 T)
Gd@C_{82}-$(OH)_{40}$[16]	81 (1 T)
Gd@C_{82}-$O_6(OH)_{16}(NHCH_2CH_2COOH)_8$[90a]	9.1 (1.5 T), 8.1 (0.35 T)
Gd@C_{82}-$O_6(OH)_{16}(NHCH_2CH_2CO$-antiGFP$)_5$[90b]	12 (0.35 T)
$Gd_3N@C_{80}$-[DIPEG5000$(OH)_x$][90c]	102 (0.35 T), 143 (2.4 T), 32 (9.4 T)
$ScGd_2N@C_{80}$-$O_{12}(OH)_{26}$[90d]	20.7 (14.1 T)
$Sc_2GdN@C_{80}$-$O_{12}(OH)_{26}$[90d]	17.6 (14.1 T)
Gd-DTPA[152]	3.9 (1 T)

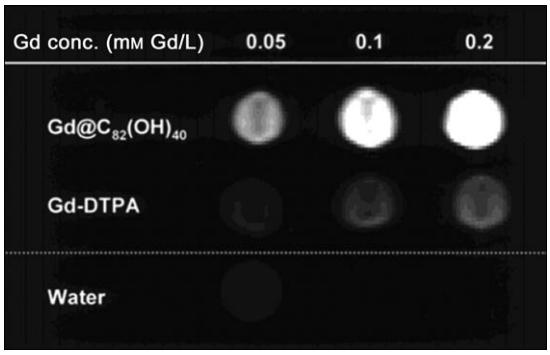

Figure 14. Enhancement of the MRI signals by Gd@$C_{82}(OH)_{40}$ compared to Gd-DTPA and water under the same conditions. Reproduced with permission from Ref. [16]. Copyright 2001 American Chemical Society.

Polyethylene glycol (PEG) derivatives of $Gd_3N@C_{80}$ ($Gd_3N@C_{80}$-[DIPEG5000$(OH)_x$]) showed even better relaxivities than $Gd@C_{82}$ derivatives. Besides the higher number of gadolinium atoms inside the carbon cage, two other factors were shown to be critical: 1) the interaction between water and the endohedral paramagnetic metals can be improved and 2) the aggregation properties of these compounds can be enhanced.[14,90c,153] However, the very low yield of $Gd_3N@C_{80}$ is a serious limitation to the commercial development of this system. Therefore, the more easily prepared mixed metallic nitride EMFs $Sc_xGd_{3-x}N@C_{80}$ were recently investigated.[90d] Even though their relaxivities are lower than that of $Gd_3N@C_{80}$, these compounds are still potentially useful as alternatives to the commercially available Gd^{III} chelates (Table 13). Another interesting application of the mixed metallic nitride EMFs is that they could lead to multifunctional contrast agents for X-ray and MRI.[154] Gd is good for MRI applications, while Lu and Ho, for example, provide good X-ray contrast.

The recent synthesis of new trimetallic nitride EMFs, with larger cages and other paramagnetic metals such as Nd, Pr, and Ce should lead to an even larger number of compounds suitable for medical imaging. A very interesting article recently reported that the coupling of $Gd@C_{82}$-$O_6(OH)_{16}(NHCH_2CH_2COOH)_8$ to the antibody of the green fluorescent protein (anti-GFP)[90b] resulted in higher relaxivity efficiencies (Table 13). The future coupling of gadolinium endohedral fullerides to tumor antibodies could, therefore, help in the early diagnosis of tumors.

The therapeutic use of water-soluble EMFs, which has been considered for a long time,[15] could become a reality with the recent report of their ability to scavenge reacting oxygen species (ROS).[155] $Gd@C_{82}(OH)_{22}$ showed a higher capacity than $C_{60}(OH)_{22}$ and $C_{60}(C(COOH)_2)_2$ to scavenge the superoxide radical anion ($O_2^{\bullet-}$), the hydroxyl radical ($HO^{\bullet}$), and singlet oxygen. The reason for this finding is presumably the higher electron affinity of $Gd@C_{82}$ than C_{60}. As these reactive oxygen species are the mediators of oxidative stress, which is linked to diseases as varied as cancer, HIV, and athereosclerosis, the therapeutic potential of EMFs looks very promising. Additionally, EMFs could be suitable for radioimmunotherapy, since their carbon cages prevent the leakage of radionuclides into organs. Diener et al. recently reported the encapsulation of α-emitting radionuclides such as ^{212}Pb and ^{213}Bi in C_{60}, and the exohedral functionalization of the resulting EMFs.[67] Preliminary studies in mice confirmed that ^{212}Pb did not accumulate in bones.

6. Summary and Outlook

Endohedral metallofullerenes combine the metallic properties of the incarcerated moiety with the properties of the fullerene host. The interaction between the metal cluster and the carbon cage is mostly ionic, since there is electron transfer from the encapsulated moiety to the carbon cage. This electron transfer accounts for the stability and most of their electronic properties of EMFs. So far, several types of EMFs have been synthesized, which include those with encapsulated single and multiple metal atoms (classical EMFs), metallic carbides, trimetallic nitrides, and metal oxides. Of these, the trimetallic nitride family is the largest. To date metals from group III and lanthanides have been found to form trimetallic nitride EMFs, thus offering a broad variety of metals with properties suitable for potential use in different fields. One of the most interesting properties of EMFs is the strong interaction between the entrapped metal(s) and the carbon cage, this interaction accounts for the formation of carbon cages that have never been isolated independently. For example, many violations of the IPR rule have been reported for EMFs.

Chemical functionalization has also revealed that EMFs are chemically different from empty cages. It seems that the metal cluster has a considerable influence on the carbon cage, making certain bonds more reactive towards some reactions. However, the low yields of some EMFs and the difficulty of isolating and purifying mono- and bisadducts have restrained progress in this field. On the other hand, functionalized and nonfunctionalized EMFs have interesting electrochemical properties that expand the number of possible applications.

Even though there have been many significant contributions to the field of EMF research, there are still many questions that need to be addressed in the near future, such as: What is the influence of the metal on the carbon cage? What are the rules of stabilization for non-IPR EMFs? Which other types of endohedral confinement are possible? How can the selective synthesis of EMFs be controlled and how can their yields be increased? Clearly the EMF field remains a fascinating, challenging, and still largely unexplored arena with many potential applications.

Financial support from the National Science Foundation (Grant number DMR-0809129) is greatly appreciated. This material is based on work supported by the National Science Foundation while L.E. was working there. All opinions, findings, conclusions, or recommendations expressed herein are those of the authors and do not necessarily reflect the views of the National Science Foundation.

Received: April 1, 2009

[1] J. R. Heath, S. C. O'Brien, Q. Zhang, Y. Liu, R. F. Curl, H. W. Kroto, F. K. Tittel, R. E. Smalley, *J. Am. Chem. Soc.* **1985**, *107*, 7779–7780.
[2] H. Shinohara, *Rep. Prog. Phys.* **2000**, *63*, 843–892.
[3] S. Nagase, K. Kobayashi, T. Akasaka, T. Wakahara in *Fullerenes: Chemistry, Physics and Technology* (Eds.: K. M. Kadish, R. S. Ruoff), Wiley, New York, **2000**, chap. 9, pp. 96–436.
[4] S. Liu, S. Sun, *J. Organomet. Chem.* **2000**, *599*, 74–86.
[5] *Endofullerenes: A New Family of Carbon Clusters* (Ed.: T. Akasaka, S. Nagase), Kluwer, Dordrecht, **2002**.
[6] R. Kitaura, H. Shinohara, *Jpn. J. Appl. Phys. Part 1* **2007**, *46*, 881–891.
[7] L. Dunsch, S. Yang, *Phys. Chem. Chem. Phys.* **2007**, *9*, 3067–3081.
[8] L. Dunsch, S. Yang, *Small* **2007**, *3*, 1298–1320.
[9] M. N. Chaur, A. J. Athans, L. Echegoyen, *Tetrahedron* **2008**, *64*, 11387–11393.

[10] S. Stevenson, M. A. Mackey, M. A. Stuart, J. P. Phillips, M. L. Easterling, C. J. Chancellor, M. M. Olmstead, A. L. Balch, *J. Am. Chem. Soc.* **2008**, *130*, 11844 – 11845.

[11] a) M. Saunders, H. A. Jimenez-Vazquez, R. J. Cross, R. J. Poreda, *Science* **1993**, *259*, 1428 – 1430; b) M. Saunders, H. A. Jimenez-Vazquez, R. J. Cross, M. Mroczkowski, M. L. Gross, D. E. Giblin, R. J. Poreda, *J. Am. Chem. Soc.* **1994**, *116*, 2193 – 2194; c) M. S. Syamala, R. J. Cross, M. Saunders, *J. Am. Chem. Soc.* **2002**, *124*, 6216 – 6219.

[12] H. Mauser, A. Hirsch, N. J. R. van Eikema Hommes, T. Clark, B. Pietzak, A. Weidinger, L. Dunsch, *Angew. Chem.* **1997**, *109*, 2858 – 2861; *Angew. Chem. Int. Ed. Engl.* **1997**, *36*, 2835 – 2838.

[13] J. A. Larsson, J. C. Greer, W. Harneit, A. Weidinger, *J. Chem. Phys.* **2002**, *116*, 7849 – 7854.

[14] R. D. Bolskar, *Nanomedicine* **2008**, *3*, 201 – 213.

[15] V. K. Koltover, *Progress in Fullerene Research*, Nova Science, Hauppauge, **2007**, p. 199.

[16] M. Mikawa, H. Kato, M. Okumura, M. Narazaki, Y. Kanazawa, N. Miwa, H. Shinohara, *Bioconjugate Chem.* **2001**, *12*, 510 – 514.

[17] H. Kato, Y. Yanazawa, M. Okumura, A. Taninaka, T. Yokawa, H. Shinohara, *J. Am. Chem. Soc.* **2003**, *125*, 4391 – 4397.

[18] R. D. Bolskar, A. F. Benedetto, L. O. Husebo, R. E. Price, E. F. Jackson, S. Wallace, L. J. Wilson, J. M. Alford, *J. Am. Chem. Soc.* **2003**, *125*, 5471 – 5478.

[19] S. Laus, B. Sitharaman, E. Toth, R. D. Bolskar, L. Helm, S. Asokan, M. S. Wong, L. J. Wilson, A. E. Merbach, *J. Am. Chem. Soc.* **2005**, *127*, 9368 – 9369.

[20] S. F. Yang, L. Z. Fan, S. H. Yang, *Chem. Phys. Lett.* **2004**, *388*, 253 – 258.

[21] J. R. Pinzon, M. E. Plonska-Brzezinska, C. M. Cardona, A. J. Athans, S. S. Gayathri, D. M. Guldi, M. A. Herranz, N. Martin, T. Torres, L. Echegoyen, *Angew. Chem.* **2008**, *120*, 4241 – 4244; *Angew. Chem. Int. Ed.* **2008**, *47*, 4173 – 4176.

[22] J. Tang, G. Xing, Y. Zhao, L. Jing, H. Yuan, F. Zhao, X. Gao, H. Qian, R. Su, K. Ibrahim, W. Chu, L. Zhang, K. Tanigaki, *J. Phys. Chem. B* **2007**, *111*, 11929 – 11934.

[23] J. Lee, H. Kim, S. J. Kahng, G. Kim, Y. W. Son, J. Ihm, H. Kato, Z. W. Wang, T. Okazaki, H. Shinohara, Y. Kuk, *Nature* **2002**, *415*, 1005 – 1008.

[24] T. Okazaki, T. Shimada, K. Suenaga, Y. Ohno, T. Mizutani, J. Lee, Y. Kuk, H. Shinohara, *Appl. Phys. A* **2003**, *76*, 475 – 478.

[25] J. H. Warner, A. A. R. Watt, L. Ge, K. Porfyrakis, T. Akachi, H. Okimoto, Y. Ito, A. Ardavan, B. Montanari, J. H. Jefferson, N. M. Harrison, H. Shinohara, G. A. D. Briggs, *Nano Lett.* **2008**, *8*, 1005 – 1010.

[26] M. Kalbac, L. Kavan, M. Zukalova, S. F. Yang, J. Cech, S. Roth, L. Dunsch, *Chem. Eur. J.* **2007**, *13*, 8811 – 8817.

[27] Y. Chai, T. Guo, C. Jin, R. E. Haufler, L. P. F. Chibante, J. Fure, L. Wang, G. M. Alford, R. E. Smalley, *J. Phys. Chem.* **1991**, *95*, 7564 – 7568.

[28] a) P. W. Fowler, D. E. Monolopoulos, *An Atlas of Fullerenes*, Clarendon, Oxford, **1995**; b) K. Kobayashi, S. Nagase, M. Yoshida, E. Osawa, *J. Am. Chem. Soc.* **1997**, *119*, 12693 – 12694.

[29] a) K. Kobayashi, S. Nagase, Y. Maeda, T. Wakahara, T. Akasaka, *Chem. Phys. Lett.* **2003**, *374*, 562 – 566; b) É. Tóth, R. D. Bolskar, A. Borel, G. González, L. Helm, A. E. Merbach, B. Sitharaman, L. J. Wilson, *J. Am. Chem. Soc.* **2005**, *127*, 799 – 805.

[30] a) T. Akasaka, T. Kato, K. Kobayashi, S. Nagase, K. Yamamoto, H. Funasaka, T. Takahashi, *Nature* **1995**, *374*, 600 – 601; b) T. Kato, T. Akasaka, K. Kobayashi, S. Nagase, K. Kikuchi, Y. Achiba, T. Suzuki, K. Yamamoto, *J. Phys. Chem. Solids* **1997**, *58*, 1779 – 1783; c) M. Yamada, L. Feng, T. Wakahara, T. Tsuchiya, Y. Maeda, Y. Lian, M. Kako, T. Akasaka, T. Kato, K. Kobayashi, S. Nagase, *J. Phys. Chem. B* **2005**, *109*, 6049 – 6051.

[31] T. Akasaka, S. Nagase, K. Kobayashi, T. Suzuki, T. Kato, K. Yamamoto, H. Funasaka, T. Takahashi, *J. Chem. Soc. Chem. Commun.* **1995**, 1343 – 1344.

[32] T. Akasaka, T. Kato, S. Nagase, K. Kobayashi, K. Yamamoto, H. Funasaka, T. Takahashi, *Tetrahedron* **1996**, *52*, 5015 – 5020.

[33] a) T. Akasaka, S. Okubo, M. Kondo, Y. Maeda, T. Wakahara, T. Kato, T. Suzuki, K. Yamamoto, K. Kobayashi, S. Nagase, *Chem. Phys. Lett.* **2000**, *319*, 153 – 156; b) T. Wakahara, J.-I. Kobayashi, M. Yamada, Y. Maeda, T. Tsuchiya, M. Okamura, T. Akasaka, M. Waelchli, K. Kobayashi, S. Nagase, T. Kato, M. Kako, K. Yamamoto, K. M. Kadish, *J. Am. Chem. Soc.* **2004**, *126*, 4883 – 4887; c) Y. Iiduka, O. Ikenaga, A. Sakuraba, T. Wakahara, T. Tsuchiya, Y. Maeda, T. Nakahodo, T. Akasaka, M. Kako, N. Mizorogi, S. Nagase, *J. Am. Chem. Soc.* **2005**, *127*, 9956 – 9957; d) T. Wakahara, Y. Iiduka, O. Ikenaga, T. Nakahodo, A. Sakuraba, T. Tsuchiya, Y. Maeda, M. Kako, T. Akasaka, K. Yoza, E. Horn, N. Mizorogi, S. Nagase, *J. Am. Chem. Soc.* **2006**, *128*, 9919 – 9925; e) M. Yamada, T. Wakahara, T. Tsuchiya, Y. Maeda, M. Kako, T. Akasaka, K. Yoza, E. Horn, N. Mizorogi, S. Nagase, *Chem. Commun.* **2008**, 558 – 560.

[34] Y. Maeda, J. Miyashita, T. Hasegawa, T. Wakahara, T. Tsuchiya, L. Feng, Y. Lian, T. Akasaka, K. Kobayashi, S. Nagase, M. Kako, K. Yamamoto, K. M. Kadish, *J. Am. Chem. Soc.* **2005**, *127*, 2143 – 2146.

[35] a) Y. Maeda, Y. Matsunaga, T. Wakahara, S. Takahashi, T. Tsuchiya, M. O. Ishitsuka, T. Hasegawa, T. Akasaka, M. T. H. Liu, K. Kokura, E. Horn, K. Yoza, T. Kato, S. Okubo, K. Kobayashi, S. Nagase, K. Yamamoto, *J. Am. Chem. Soc.* **2004**, *126*, 6858 – 6859; b) Y, Matsunaga, Y. Maeda, T. Wakahara, T. Tsuchiya, M. O. Ishitsuka, T. Akasaka, N. Mizorogi, K. Kobayashi, S. Nagase, K. M. Kadish, *ITE Lett.* **2006**, *7*, C1.

[36] Y. Iiduka, T. Wakahara, T. Nakahodo, T. Tsuchiya, A. Sakuraba, Y. Maeda, T. Akasaka, K. Yoza, E. Horn, T. Kato, M. T. H. Liu, N. Mizorogi, K. Kobayashi, S. Nagase, *J. Am. Chem. Soc.* **2005**, *127*, 12500 – 12501.

[37] Y. Iiduka, T. Wakahara, K. Nakajima, T. Nakahodo, T. Tsuchiya, Y. Maeda, T. Akasaka, K. Yoza, M. T. H. Liu, N. Mizorogi, S. Nagase, *Angew. Chem.* **2007**, *119*, 5658 – 5660; *Angew. Chem. Int. Ed.* **2007**, *46*, 5562 – 5564.

[38] T. Akasaka, T. Kono, Y. Matsunaga, T. Wakahara, T. Nakahodo, M. O. Ishitsuka, Y. Maeda, T. Tsuchiya, T. Kato, M. T. H. Liu, N. Mizorogi, Z. Slanina, S. Nagase, *J. Phys. Chem. A* **2008**, *112*, 1294 – 1297.

[39] T. Akasaka, T. Kono, Y. Takematsu, H. Nikawa, T. Nakahodo, T. Wakahara, M. O. Ishitsuka, T. Tsuchiya, Y. Maeda, M. T. H. Liu, K. Yoza, T. Kato, K. Yamamoto, N. Mizorogi, Z. Slanina, S. Nagase, *J. Am. Chem. Soc.* **2008**, *130*, 12840 – 12841.

[40] a) B. Cao, H. Nikawa, T. Nakahodo, T. Tsuchiya, Y. Maeda, T. Akasaka, H. Sawa, Z. Slanina, N. Mizorogi, S. Nagase, *J. Am. Chem. Soc.* **2008**, *130*, 983 – 989; b) X. Lu, H. Nikawa, T. Nakahodo, T. Tsuchiya, M. O. Ishitsuka, Y. Maeda, T. Akasaka, M. Toki, H. Sawa, Z. Slanina, N. Mizorogi, S. Nagase, *J. Am. Chem. Soc.* **2008**, *130*, 9129 – 9136; c) X. Lu, H. Nikawa, T. Tsuchiya, Y. Maeda, M. O. Ishitsuka, T. Akasaka, M. Toki, H. Sawa, Z. Slanina, N. Mizorogi, S. Nagase, *Angew. Chem.* **2008**, *120*, 8770 – 8773; *Angew. Chem. Int. Ed.* **2008**, *47*, 8642 – 8645.

[41] N. Tagmatarchis, A. Taninaka, H. Shinohara, *Chem. Phys. Lett.* **2002**, *355*, 226 – 232.

[42] C. Shu, C. Slebodnick, L. Xu, H. Champion, T. Fuhrer, T. Cai, J. E. Reid, W. Fu, K. Harich, H. C. Dorn, H. W. Gibson, *J. Am. Chem. Soc.* **2008**, *130*, 17755 – 17760.

[43] E. B. Iezzi, J. C. Duchamp, K. Harich, T. Glass, H. M. Lee, M. M. Olmstead, A. L. Balch, H. C. Dorn, *J. Am. Chem. Soc.* **2002**, *124*, 524 – 525.

[44] H. M. Lee, M. M. Olmstead, E. B. Iezzi, J. C. Duchamp, H. C. Dorn, A. L. Balch, *J. Am. Chem. Soc.* **2002**, *124*, 3494 – 3495.

[45] S. Stevenson, R. R. Stephen, T. M. Amos, V. R. Cadorette, J. E. Reid, J. P. Phillips, *J. Am. Chem. Soc.* **2005**, *127*, 12776 – 12777.
[46] Y. Maeda, J. Miyashita, T. Hasegawa, T. Wakahara, T. Tsuchiya, T. Nakahodo, T. Akasaka, N. Mizorogi, K. Kobayashi, S. Nagase, T. Kato, N. Ban, H. Nakajima, Y. Watanabe, *J. Am. Chem. Soc.* **2005**, *127*, 12190 – 12191.
[47] a) Z. Ge, J. C. Duchamp, T. Cai, H. W. Gibson, H. C. Dorn, *J. Am. Chem. Soc.* **2005**, *127*, 16292 – 16298; b) T. Cai, L. Xu, M. R. Anderson, Z. Ge, T. Zuo, X. Wang, M. M. Olmstead, A. L. Balch, H. W. Gibson, H. C. Dorn, *J. Am. Chem. Soc.* **2006**, *128*, 8581 – 8589; c) C. D. Angeli, T. Cai, J. C. Duchamp, J. C. Reid, E. S. Singer, H. W. Gibson, H. C. Dorn, *Chem. Mater.* **2008**, *20*, 4993 – 4997.
[48] S. Osuna, M. Swart, M. Solà, *J. Am. Chem. Soc.* **2009**, *131*, 129 – 139.
[49] B. Cao, T. Wakahara, Y. Maeda, A. Han, T. Akasaka, T. Kato, K. Kobayashi, S. Nagase, *Chem. Eur. J.* **2004**, *10*, 716 – 720.
[50] X. Lu, X. He, L. Feng, Z. Shi, Z. Gu, *Tetrahedron* **2004**, *60*, 3713 – 3716.
[51] L. Feng, X. Lu, X. He, Z. Shi, Z. Gu, *Inorg. Chem. Commun.* **2004**, *7*, 1010 – 1013.
[52] H. C. Dorn, E. B. Iezzi, J. Duchamp, U.S. Patent Application 20040054151, March 18, **2004**.
[53] C. M. Cardona, A. Kitaygorodskiy, A. Ortiz, M. A. Herranz, L. Echegoyen, *J. Org. Chem.* **2005**, *70*, 5092 – 5097.
[54] C. M. Cardona, A. Kitaygorodskiy, L. Echegoyen, *J. Am. Chem. Soc.* **2005**, *127*, 10448 – 10453.
[55] T. Cai, Z. Ge, E. B. Iezzi, T. E. Glass, K. Harich, H. W. Gibson, H. C. Dorn, *Chem. Commun.* **2005**, 3594 – 3596.
[56] M. Yamada, T. Wakahara, T. Nakahodo, T. Tsuchiya, Y. Maeda, T. Akasaka, K. Yoza, E. Horn, N. Mizorogi, S. Nagase, *J. Am. Chem. Soc.* **2006**, *128*, 1402 – 1403.
[57] T. Cai, C. Slebodnick, L. Xu, K. Harich, T. E. Glass, C. Chancellor, J. C. Fettinger, M. M. Olmstead, A. L. Balch, H. W. Gibson, H. C. Dorn, *J. Am. Chem. Soc.* **2006**, *128*, 6486 – 6492.
[58] C. M. Cardona, B. Elliott, L. Echegoyen, *J. Am. Chem. Soc.* **2006**, *128*, 6480 – 6485.
[59] A. Rodriguez-Fortea, J. M. Campanera, C. M. Cardona, L. Echegoyen, J. M. Poblet, *Angew. Chem.* **2006**, *118*, 8356 – 8360; *Angew. Chem. Int. Ed.* **2006**, *45*, 8176 – 8180.
[60] L. Echegoyen, C. J. Chancellor, C. M. Cardona, B. Elliott, J. Rivera, M. M. Olmstead, A. L. Balch, *Chem. Commun.* **2006**, 2653 – 2655.
[61] N. Martin, M. Altable, S. Filippone, A. Martin-Domenech, L. Echegoyen, C. M. Cardona, *Angew. Chem.* **2006**, *118*, 116 – 120; *Angew. Chem. Int. Ed.* **2006**, *45*, 110 – 114.
[62] N. Chen, E.-Y. Zhang, K. Tan, C.-R. Wang, X. Lu, *Org. Lett.* **2007**, *9*, 2011 – 2013.
[63] N. Chen, L.-Z. Fan, K. Tan, Y.-Q. Wu, C.-Y. Shu, X. Lu, C.-R. Wang, *J. Phys. Chem. C* **2007**, *111*, 11823 – 11828.
[64] T. Cai, L. Xu, H. W. Gibson, H. C. Dorn, C. J. Chancellor, M. M. Olmstead, A. L. Balch, *J. Am. Chem. Soc.* **2007**, *129*, 10795 – 10800.
[65] J. R. Pinzón, C. M. Cardona, M. A. Herranz, M. E. Plonska-Brzezinska, A. Palkar, A. J. Athans, N. Martin, A. Rodriguez-Fortea, J. M. Poblet, G. Bottari, T. Torres, S. S. Gayathri, D. M. Guldi, L. Echegoyen, *Chem. Eur. J.* **2009**, *15*, 864 – 877.
[66] R. D. Bolskar, A. F. Benedetto, L. O. Husebo, R. E. Price, E. F. Jackson, S. Wallace, L. J. Wilson, J. M. Alford, *J. Am. Chem. Soc.* **2003**, *125*, 5471 – 5478.
[67] M. D. Diener, J. M. Alford, S. J. Kennel, S. Mirzadeh, *J. Am. Chem. Soc.* **2007**, *129*, 5131 – 5138.
[68] L. Feng, T. Nakahodo, T. Wakahara, T. Tsuchiya, Y. Maeda, T. Akasaka, T. Kato, E. Horn, K. Yoza, N. Mizorogi, S. Nagase, *J. Am. Chem. Soc.* **2005**, *127*, 17136 – 17137.
[69] a) L. Feng, T. Wakahara, T. Nakahodo, T. Tsuchiya, Q. Piao, Y. Maeda, Y. Lian, T. Akasaka, E. Horn, K. Yoza, T. Kato, N. Mizorogi, S. Nagase, *Chem. Eur. J.* **2006**, *12*, 5578 – 5586; b) L. Feng, T. Tsuchiya, T. Wakahara, T. Nakahodo, Q. Piao, Y. Maeda, T. Akasaka, T. Kato, K. Yoza, E. Horn, N. Mizorogi, S. Nagase, *J. Am. Chem. Soc.* **2006**, *128*, 5990 – 5991.
[70] M. A. Herranz, F. Diederich, L. Echegoyen, *Eur. J. Org. Chem.* **2004**, 2299 – 2316.
[71] O. Lukoyanova, C. M. Cardona, J. Rivera, L. Z. Lugo-Morales, C. J. Chancellor, M. M. Olmstead, A. Rodríguez-Fortea, J. M. Poblet, A. L. Balch, L. Echegoyen, *J. Am. Chem. Soc.* **2007**, *129*, 10423 – 10430.
[72] M. N. Chaur, F. Melin, A. J. Athans, B. Elliott, K. Walker, B. C. Holloway, L. Echegoyen, *Chem. Commun.* **2008**, 2665 – 2667.
[73] T. Cai, L. Xu, C. Shu, H. A. Champion, J. E. Reid, C. Anklin, M. R. Anderson, H. W. Gibson, H. C. Dorn, *J. Am. Chem. Soc.* **2008**, *130*, 2136 – 2137.
[74] T. Suzuki, Y. Maruyama, T. Kato, T. Akasaka, K. Yamamoto, H. Funasaka, T. Takahashi, *J. Am. Chem. Soc.* **1995**, *117*, 9606 – 9607.
[75] a) H. Nikawa, T. Kikuchi, T. Wakahara, T. Nakahodo, T. Tsuchiya, G. M. A. Rahman, T. Akasaka, Y. Maeda, K. Yoza, E. Horn, K. Yamamoto, N. Mizorogi, S. Nagase, *J. Am. Chem. Soc.* **2005**, *127*, 9684 – 9685; b) T. Wakatsugu, H. Nikawa, T. Kikuchi, T. Nakahodo, G. M. A. Rahman, T. Tsuchiya, Y. Maeda, T. Akasaka, K. Yoza, E. Horn, K. Yamamoto, N. Mizorogi, Z. Slanina, S. Nagase, *J. Am. Chem. Soc.* **2006**, *128*, 14228 – 14229.
[76] I. E. Kareev, S. F. Lebedkin, V. P. Bubnov, E. B. Yagubskii, I. N. Ioffe, P. A. Khavrel, I. V. Kuvychko, S. H. Strauss, O. V. Boltalina, *Angew. Chem.* **2005**, *117*, 1880 – 1883; *Angew. Chem. Int. Ed.* **2005**, *44*, 1846 – 1849.
[77] Y. Takano, A. Yomogida, H. Nikawa, M. Yamada, T. Wakahara, T. Tsuchiya, M. O. Ishitsuka, Y. Maeda, T. Akasaka, T. Kato, Z. Slanina, N. Mizorogi, S. Nagase, *J. Am. Chem. Soc.* **2008**, *130*, 16224 – 16230.
[78] N. B. Shustova, A. A. Popov, M. A. Mackey, C. E. Coumbe, J. P. Phillips, S. Stevenson, S. H. Strauss, O. V. Boltalina, *J. Am. Chem. Soc.* **2007**, *129*, 11676 – 11677.
[79] C. Shu, T. Cai, L. Xu, T. Zuo, J. Reid, K. Harich, H. C. Dorn, H. W. Gibson, *J. Am. Chem. Soc.* **2007**, *129*, 15710 – 15717.
[80] C. Hao, Z. Liu, X. Guo, Z. Liu, W. Xu, Y. Sun, S. Liu, *Rapid Commun. Mass Spectrom.* **1997**, *11*, 1677 – 1680.
[81] a) L. Feng, X. Zhang, Z. Yu, J. Wang, Z. Gu, *Chem. Mater.* **2002**, *14*, 4021 – 4022; b) X. Lu, J. Xu, X. He, Z. Shi, Z. Gu, *Chem. Mater.* **2004**, *16*, 953 – 955.
[82] X. Li, L. Fan, D. Liu, H. H. Y. Sung, I. D. Williams, S. Yang, K. Tan, Xin Lu, *J. Am. Chem. Soc.* **2007**, *129*, 10636 – 10637.
[83] S. Zhang, D. Sun, X. Li, F. Pei, S. Liu, *Fullerene Sci. Technol.* **1997**, *5*, 1635 – 1643.
[84] a) L. J. Wilson, D. W. Cagle, T. P. Thrash, S. J. Kennel, S. Mirzadeh, J. M. Alford, G. J. Ehrhardt, *Coord. Chem. Rev.* **1999**, *190–192*, 199 – 207; b) D. W. Cagle, S. J. Kennel, S. Mirzadeh, J. M. Alford, L. J. Wilson, *Proc. Natl. Acad. Sci. USA* **1999**, *96*, 5182 – 5187.
[85] D. Sun, H. Huang, S. Yang, Z. Liu, S. Liu, *Chem. Mater.* **1999**, *11*, 1003 – 1006.
[86] a) H. Kato, K. Suenaga, M. Mikawa, M. Okumura, N. Miwa, A. Yashiro, H. Fujimura, A. Mizuno, Y. Nishida, K. Kobayashi, H. Shinohara, *Chem. Phys. Lett.* **2000**, *324*, 255 – 259; b) H. Kato, Y. Kanazawa, M. Okumura, A. Taninaka, T. Yokawa, H. Shinohara, *J. Am. Chem. Soc.* **2003**, *125*, 4391 – 4397.
[87] E. B. Iezzi, F. Cromer, P. Stevenson, H. C. Dorn, *Synth. Met.* **2002**, *128*, 289 – 291.
[88] X. Lu, X. Zhou, Z. Shi, Z. Gu, *Inorg. Chim. Acta* **2004**, *357*, 2397 – 2400.
[89] Y. Zhang, J. Xiang, J. Zhuang, Y. Li, B. Xin, F. Liu, K. Hou, Y. Tang, *Chem. Lett.* **2005**, *34*, 1264 – 1265.

[90] a) C.-Y. Shu, L.-H. Gan, C.-R. Wang, X.-l. Pei, H.-b. Han, *Carbon* **2006**, *44*, 496 – 500; b) C.-Y. Shu, X.-Y. Ma, J.-F. Zhang, F. D. Corwin, J. H. Sim, E.-Y. Zhang, H. C. Dorn, H. W. Gibson, P. P. Fatouros, C.-R. Wang, X.-H. Fang, *Bioconjugate Chem.* **2008**, *19*, 651 – 655; c) P. P. Fatouros, F. D. Corwin, Z.-J. Chen, W. C. Broaddus, J. L. Tatum, B. Kettenmann, Z. Ge, H. W. Gibson, J. L. Russ, A. P. Leonard, J. C. Duchamp, H. C. Dorn, *Radiology* **2006**, *240*, 756 – 764; d) E.-Y. Zhang, C.-Y. Shu, L. Feng, C.-R. Wang, *J. Phys. Chem. B* **2007**, *111*, 14223 – 14226.

[91] H. Kroto, J. R. Heath, S. C. O'Brien, R. F. Curl, R. F. Smalley, *Nature* **1985**, *318*, 162 – 163.

[92] a) W. Krätschmer, K. Fostiropoulos, D. R. Huffman, *Chem. Phys. Lett.* **1990**, *170*, 167 – 170; b) W. Krätschmer, W. Fostiropoulos, L. D. Lamb, D. R. Huffman, *Nature* **1990**, *347*, 354 – 358.

[93] S. Stevenson, G. Rice, T. Glass, K. Harish, F. Cromer, M. R. Jordan, J. Kraft, E. Hadju, R. Bible, M. M. Olmstead, K. Maitra, A. J. Fisher, A. L. Balch, H. C. Dorn, *Nature* **1999**, *401*, 55 – 57.

[94] L. Dunsch, M. Krause, J. Noack, P. Georgi, *J. Phys. Chem. Solids* **2004**, *65*, 309 – 315.

[95] M. Takata, B. Umeda, E. Nishibori, M. Sakata, Y. Saitot, M. Ohno, H. Shinohara, *Nature* **1995**, *377*, 46 – 49.

[96] C. R. Wang, T. Kai, T. Tomiyama, T. Yoshida, Y. Kobayashi, E. Nishibori, M. Takata, M. Sakata, H. Shinohara, *Angew. Chem.* **2001**, *113*, 411 – 413; *Angew. Chem. Int. Ed.* **2001**, *40*, 397 – 399.

[97] C. R. Wang, M. Inakuma, H. Shinohara, *Chem. Phys. Lett.* **1999**, *300*, 379 – 384.

[98] T. Inoue, T. Tomiyama, T. Sugai, H. Shinohara, *Chem. Phys. Lett.* **2003**, *382*, 226 – 231.

[99] T. Inoue, T. Tomiyama, T. Sugai, T. Okasaki, T. Suematsu, N. Fujii, H. Utsumi, K. Nojima, H. Shinohara, *J. Phys. Chem. B* **2004**, *108*, 7573 – 7579.

[100] K. Tan, X. Lu, *Chem. Commun.* **2005**, 4444 – 4446.

[101] T. Yumura, Y. Satu, K. Suenaga, S. Iijima, *J. Phys. Chem. B* **2005**, *109*, 20251 – 20255.

[102] K. Tan, X. Lu, *J. Phys. Chem. A* **2006**, *110*, 1171 – 1176.

[103] Y. Sato, T. Yumura, K. Suenaga, H. Moribe, D. Nishide, M. Ishida, H. Shinohara, *Phys. Rev. B* **2006**, *73*, 193401.

[104] Z. Q. Shi, X. Wu, C. R. Wang, X. Lu, H. Shinohara, *Angew. Chem.* **2006**, *118*, 2161 – 2165; *Angew. Chem. Int. Ed.* **2006**, *45*, 2107 – 2111.

[105] Y. Iiduka, T. Wakahara, K. Nakajima, T. Tsuchiya, T. Nakahodo, Y. Maeda, T. Akasaka, N. Mizorogi, S. Nagase, *Chem. Commun.* **2006**, 2057 – 2059.

[106] H. Yang, C. Lu, Z. Liu, H. Jin, Y. Che, M. M. Olmstead, A. L. Balch, *J. Am. Chem. Soc.* **2008**, *130*, 17296 – 17300.

[107] Y. Yamazaki, K. Nakajima, T. Wakahara, T. Tsuchiya, M. O. Ishitsuka, Y. Maeda, T. Akasaka, M. Waelchli, N. Mizorogi, S. Nagase, *Angew. Chem.* **2008**, *120*, 8023 – 8026; *Angew. Chem. Int. Ed.* **2008**, *47*, 7905 – 7908.

[108] H. Shinohara, M. Inakuma, N. Hayashi, H. Sato, Y. Saito, T. Kato, S. Bandow, *J. Phys. Chem.* **1994**, *98*, 8597 – 8599.

[109] R. Valencia, A. Rodriguez-Fortea, J. M. Poblet, *J. Phys. Chem. A* **2008**, *112*, 4550 – 4555.

[110] S. Stevenson, P. W. Fowler, T. Heine, J. C. Duchamp, G. Rice, T. Glass, K. Harich, E. Hajdu, R. Bible, H. C. Dorn, *Nature* **2000**, *408*, 427 – 428.

[111] J. M. Campanera, C. Bo, J. M. Poblet, *Angew. Chem.* **2005**, *117*, 7396 – 7399; *Angew. Chem. Int. Ed.* **2005**, *44*, 7230 – 7233.

[112] a) A. A. Popov, L. Dunsch, *J. Am. Chem. Soc.* **2007**, *129*, 11835 – 11849; b) A. A. Popov, L. Dunsch, *J. Am. Chem. Soc.* **2008**, *130*, 17726 – 17746.

[113] M. N. Chaur, F. Melin, J. Ashby, B. Elliot, A. Kumbhar, A. M. Rao, L. Echegoyen, *Chem. Eur. J.* **2008**, *14*, 8213 – 8219.

[114] a) F. Melin, M. N. Chaur, S. Engmann, B. Elliott, A. Kumbhar, A. J. Athans, L. Echegoyen, *Angew. Chem.* **2007**, *119*, 9190 – 9193; *Angew. Chem. Int. Ed.* **2007**, *46*, 9032 – 9035; b) M. N. Chaur, F. Melin, B. Elliott, A. Kumbhar, A. J. Athans, L. Echegoyen, *Chem. Eur. J.* **2008**, *14*, 4594 – 4599.

[115] C. R. Wang, T. Kai, T. Tomiyama, T. Yoshida, Y. Kobayashi, E. Nishibori, M. Takata, M. Sakata, H. Shinohara, *Nature* **2000**, *408*, 426 – 427.

[116] B. Q. Mercado, C. M. Beavers, M. M. Olmstead, M. N. Chaur, K. Walker, B. C. Holloway, L. Echegoyen, A. L. Balch, *J. Am. Chem. Soc.* **2008**, *130*, 7854 – 7855.

[117] C. M. Beavers, T. Zuo, J. C. Duchamp, K. Harich, H. C. Dorn, M. M. Olmstead, A. L. Balch, *J. Am. Chem. Soc.* **2006**, *128*, 11352 – 11353.

[118] T. Zuo, K. Walker, M. M. Olmstead, F. Melin, B. C. Holloway, L. Echegoyen, H. C. Dorn, M. N. Chaur, C. J. Chancellor, C. M. Beavers, A. L. Balch, A. J. Athans, *Chem. Commun.* **2008**, 1067 – 1069.

[119] S. Yang, A. A. Popov, L. Dunsch, *Angew. Chem.* **2007**, *119*, 1278 – 1281; *Angew. Chem. Int. Ed.* **2007**, *46*, 1256 – 1259.

[120] S. Yang, A. A. Popov, L. Dunsch, *J. Phys. Chem. B* **2007**, *111*, 13659 – 13663.

[121] H. Kato, A. Taninaka, T. Sugai, H. Shinohara, *J. Am. Chem. Soc.* **2003**, *125*, 7782 – 7783.

[122] A. A. Popov, M. Krause, S. Yang, J. Wong, L. Dunsch, *J. Phys. Chem. B* **2007**, *111*, 3363 – 3369.

[123] M. Yamada, T. Wakahara, T. Tsuchiya, Y. Maeda, T. Akasaka, N. Mizorogi, S. Nagase, *J. Phys. Chem. A* **2008**, *112*, 7627 – 7631.

[124] a) Y. Lian, Z. Shi, X. Zhou, Z. Gu, *Chem. Mater.* **2004**, *16*, 1704 – 1714; b) V. P. Bubnov, E. E. Laukhina, I. E. Kareev, V. K. Koltover, T. G. Prokhorova, E. B. Yagubskii, Y. P. Kozmin, *Chem. Mater.* **2002**, *14*, 1004 – 1008; c) T. Kodama, K. Higashi, T. Ichikawa, S. Suzuki, H. Nishikawa, I. Ikemoto, K. Kikuchi, Y. Achiba, *Chem. Lett.* **2005**, *34*, 464 – 465; d) R. D. Bolskar, J. M. Alford, *Chem. Commun.* **2003**, 1292 – 1293; e) B. Sun, Z. Gu, *Chem. Lett.* **2002**, 1164 – 1165; f) B. Sun, L. Feng, Z. Shi, Z. Gu, *Carbon* **2002**, *40*, 1591 – 1595; g) M. D. Diener, J. M. Alford, *Nature* **1998**, *393*, 668 – 671; h) D. Fuchs, H. Rietschel, R. H. Michel, A. Fischer, P. Weis, M. M. Kappes, *J. Phys. Chem.* **1996**, *100*, 725 – 729; i) T. Tsuchiya, T. Wakahara, S. Shirakura, Y. Maeda, T. Akasaka, K. Kobayashi, S. Nagase, T. Kato, K. M. Kadish, *Chem. Mater.* **2004**, *16*, 4343 – 4346; j) T. Tsuchiya, T. Wakahara Y. Lian, Y. Maeda, T. Akasaka, T. Kato, N. Mizorogi, S. Nagase, *J. Phys. Chem. B* **2006**, *110*, 22517 – 22520.

[125] B. Elliott, L. Yu, L. Echegoyen, *J. Am. Chem. Soc.* **2005**, *127*, 10885 – 10888.

[126] a) S. Stevenson, K. Harich, H. Yu, R. R. Stephen, D. Heaps, C. Coumbe, J. P. Phillips, *J. Am. Chem. Soc.* **2006**, *128*, 8829 – 8835; b) S. Stevenson, M. A. Mackey, C. E. Coumbe, J. P. Phillips, B. Elliott, L. Echegoyen, *J. Am. Chem. Soc.* **2007**, *129*, 6072 – 6073.

[127] a) S. Stevenson, M. C. Thompson, H. L. Coumbe, M. A. Mackey, C. E. Coumbe, J. P. Phillips, *J. Am. Chem. Soc.* **2007**, *129*, 16257 – 16262; b) S. Stevenson, M. A. Mackey, M. Thompson, H. L. Coumbe, P. K. Madasu, C. E. Coumbe, J. P. Phillips, *Chem. Commun.* **2007**, 4263 – 4265.

[128] M. Krause, L. Dunsch, *ChemPhysChem* **2004**, *5*, 1445 – 1449.

[129] a) T. Suzuki, Y. Maruyama, T. Kato, K. Kikuchi, Y. Achiba, *J. Am. Chem. Soc.* **1993**, *115*, 11006 – 11007; b) T. Suzuki, Y. Maruyama, T. Kato, K. Kikuchi, Y. Achiba, K. Yamamoto, H. Funasaka, T. Takahashi, *Proc. Electrochem. Soc.* **1994**, *94–24*, 1077 – 1086; c) K. Yamamoto, H. Funasaka, T. Takahashi, T. Akasaka, *J. Phys. Chem.* **1994**, *98*, 2008 – 2011; d) K. Kikuchi, Y. Nakao, S. Suzuki, Y. Achiba, T. Suzuki, Y. Maruyama, *J. Am. Chem. Soc.* **1994**, *116*, 9367 – 9368; e) T. Suzuki, K. Kikuchi, Y. Nakao, S. Suzuki, Y. Achiba, K. Yamamoto, H. Funasaka, T. Takahashi, *Proc. Electrochem. Soc.* **1995**, *95–10*, 259 – 266; f) T. Suzuki, Y. Maruyama, T. Kato, *Synth. Met.* **1995**, *70*, 1443 – 1446; g) U. Kirbach, L. Dunsch, *Angew. Chem. Int. Ed. Engl.* **1996**, *35*, 2380 – 2383; h) T. Suzuki, K. Kikuchi, F. Oguri, Y.

Nakao, S. Suzuki, Y. Achiba, K. Yamamoto, H. Funasaka, T. Takahashi, *Tetrahedron* **1996**, *52*, 4973 – 4982; i) W. Wang, J. Ding, S. Yang, X.-Y. Li, *Proc. Electrochem. Soc.* **1997**, *97–14*, 417 – 428; j) L. Dunsch, U. Kirbach, P. Kuran, *Proc. Electrochem. Soc.* **1997**, *97–42*, 761 – 771; k) T. Akasaka, S. Okubo, T. Wakahara, K. Yamamoto, T. Kato, T. Suzuki, S. Nagase, K. Kobayashi, *Proc. Electrochem. Soc.* **1999**, *99–12*, 771 – 778; l) B. Sun, M. Li, H. Luo, Z. Shi, Z. Gu, *Electrochim. Acta* **2002**, *47*, 3545 – 3549.

[130] J. Xu, M. Li, Z. Shi, Z. Gu, *Chem. Eur. J.* **2006**, *12*, 562 – 567.

[131] Y. Zhang, J. Xu, C. Hao, Z. Shi, Z. Gu, *Carbon* **2006**, *44*, 475 – 479.

[132] P. B. Burbank, J. R. Gibson, H. C. Dorn, M. R. Anderson, *J. Electroanal. Chem.* **1996**, *417*, 1 – 4.

[133] a) K. Kikuchi, S. Suzuki, Y. Nakao, N. Nakahara, T. Wakabayashi, H. Shiromaru, K. Saito, I. Ikemoto, Y. Achiba, *Chem. Phys. Lett.* **1993**, *216*, 67 – 71; b) K. Yamamoto, H. Funasaka, T. Takahasi, T. Akasaka, T. Suzuki, Y. Maruyama, *J. Phys. Chem.* **1994**, *98*, 12831 – 12833; c) T. Suzuki, Y. Maruyama, T. Kato, K. Kikuchi, Y. Nakao, Y. Achiba, K. Kobayashi, S. Nagase, *Angew. Chem.* **1995**, *107*, 1228 – 1230; *Angew. Chem. Int. Ed. Engl.* **1995**, *34*, 1094 – 1096.

[134] a) T. Akasaka, T. Wakahara, S. Nagase, K. Kobayashi, M. Waelchli, K. Yamamoto, M. Kondo, S. Shirakura, S. Okubo, Y. Maeda, T. Kato, M. Kako, Y. Nakadaira, R. Nagahata, X. Gao, E. Van Caemelbecke, K. M. Kadish, *J. Am. Chem. Soc.* **2000**, *122*, 9316 – 9317; b) T. Akasaka, T. Wakahara, S. Nagase, K. Kobayashi, M. Waelchli, K. Yamamoto, M. Kondo, S. Shirakura, Y. Maeda, T. Kato, M. Kako, Y. Nakadaira, X. Gao, E. Van Caemelbecke, K. M. Kadish, *J. Phys. Chem. B* **2001**, *105*, 2971 – 2974; c) T. Wakahara, S. Okubo, M. Kondo, Y. Maeda, T. Akasaka, M. Waelchli, M. Kako, K. Kobayashi, S. Nagase, T. Kato, K. Yamamoto, X. Gao, E. Van Caemelbecke, K. M. Kadish, *Chem. Phys. Lett.* **2002**, *360*, 235 – 239.

[135] a) M. R. Anderson, H. C. Dorn, S. A. Stevenson, *Carbon* **2000**, *38*, 1663 – 1670; b) H. Kato, A. Taninaka, T. Sugai, H. Shinohara, *J. Am. Chem. Soc.* **2003**, *125*, 7782 – 7783; c) B. Cao, T. Wakahara, T. Tsuchiya, M. Kondo, Y. Maeda, G. M. Aminur Rahman, T. Akasaka, K. Kobayashi, S. Nagase, K. Yamamoto, *J. Am. Chem. Soc.* **2004**, *126*, 9164 – 9165; d) M. Yamada, T. Nakahodo, T. Wakahara, T. Tsuchiya, Y. Maeda, T. Akasaka, M. Kako, K. Yoza, E. Horn, N. Mizorogi, K. Kobayashi, S. Nagase, *J. Am. Chem. Soc.* **2005**, *127*, 14570 – 14571; e) M. Yamada, T. Wakahara, T. Tsuchiya, Y. Maeda, T. Akasaka, N. Mizorogi, S. Nagase, *J. Phys. Chem. A* **2008**, *112*, 7627 – 7631.

[136] M. Yamada, L. Feng, T. Wakahara, T. Tsuchiya, Y. Maeda, Y. F. Lian, M. Kako, T. Akasaka, T. Kato, K. Kobayashi, S. Nagase, *J. Phys. Chem. B* **2005**, *109*, 6049 – 6051.

[137] M. Yamada, C. Someya, T. Wakahara, T. Tsuchiya, Y. Maeda, T. Akasaka, K. Yoza, E. Horn, M. T. H. Liu, N. Mizorogi, S. Nagase, *J. Am. Chem. Soc.* **2008**, *130*, 1171 – 1176.

[138] a) T. Cai, L. Xu, M. R. Anderson, Z. Ge, T. Zuo, X. Wang, M. M. Olmstead, A. L. Balch, H. W. Gibson, H. C. Dorn, *J. Am. Chem. Soc.* **2006**, *128*, 8581 – 8589; b) L. Zhang, N. Chen, L. Z. Fan, C. R. Wang, S. H. Yang, *J. Electroanal. Chem.* **2007**, *608*, 15 – 21; c) M. E. Plonska-Brzezinska, A. J. Athans, J. P. Phillips, S. Stevenson, L. Echegoyen, *J. Electroanal. Chem.* **2008**, *614*, 171 – 174.

[139] P. Jakes, K.-P. Dinse, *J. Am. Chem. Soc.* **2001**, *123*, 8854 – 8855.

[140] a) S. Yang, M. Zalibera, P. Rapta, L. Dunsch, *Chem. Eur. J.* **2006**, *12*, 7848 – 7855; b) N. Chen, E. Y. Zhang, C. R. Wang, *J. Phys. Chem. B* **2006**, *110*, 13322 – 13325; c) M. N. Chaur, F. Melin, B. Elliott, A. J. Athans, K. Walker, B. C. Holloway, L. Echegoyen, *J. Am. Chem. Soc.* **2007**, *129*, 14826 – 14829; d) T. Zuo, M. M. Olmstead, C. M. Beavers, A. L. Balch, G. Wang, G. T. Yee, C. Shu, L. Xu, B. Elliott, L. Echegoyen, J. C. Duchamp, H. C. Dorn, *Inorg. Chem.* **2008**, *47*, 5234 – 5244.

[141] a) L. Alvarez, T. Pichler, P. Georgi, T. Schwieger, H. Peisert, L. Dunsch, Z. Hu, M. Knupfer, J. Fink, P. Bressler, M. Mast, M. S. Golden, *Phys. Rev. B* **2002**, *66*, 035107; b) M. Krause, X. Liu, J. Wong, T. Pichler, M. Knupfer, L. Dunsch, *J. Phys. Chem. A* **2005**, *109*, 7088 – 7093; c) H. Shiozawa, H. Rauf, T. Pichler, D. Grimm, X. Liu, M. Knupfer, M. Kalbac, S. Yang, L. Dunsch, B. Buchner, D. Batchelor, *Phys. Rev. B* **2005**, *72*, 195409.

[142] J. M. Campanera, C. Bo, M. M. Olmstead, A. L. Balch, J. M. Poblet, *J. Phys. Chem. A* **2002**, *106*, 12356 – 12364.

[143] M. N. Chaur, R. Valencia, A. Rodríguez-Fortea, J. M. Poblet, L. Echegoyen, *Angew. Chem.* **2009**, *121*, 1453 – 1456; *Angew. Chem. Int. Ed.* **2009**, *48*, 1425 – 1428.

[144] S. Yang, P. Rapta, L. Dunsch, *Chem. Commun.* **2007**, 189 – 191.

[145] S. Yang, M. Kalbac, A. Popov, L. Dunsch, *Chem. Eur. J.* **2006**, *12*, 7856 – 7863.

[146] P. Rapta, A. A. Popov, S. Yang, L. Dunsch, *J. Phys. Chem. A* **2008**, *112*, 5858 – 5865.

[147] R. Valencia, A. Rodriguez-Fortea, J. M. Poblet, *Chem. Commun.* **2007**, 4161 – 4163.

[148] O. Lukoyanova, C. M. Cardona, M. Altable, S. Filippone, Á. Martín Domenech, N. Martín, L. Echegoyen, *Angew. Chem.* **2006**, *118*, 7590 – 7593; *Angew. Chem. Int. Ed.* **2006**, *45*, 7430 – 7433.

[149] T. Wakahara, A. Sakuraba, Y. Iiduka, M. Okamura, T. Tsuchiya, Y. Maeda, T. Akasaka, S. Okubo, T. Kato, K. Kobayashi, S. Nagase, K. M. Kadish, *Chem. Phys. Lett.* **2004**, *398*, 553 – 556.

[150] a) H. Huang, G. Gu, S. Yang, J. Fu, P. Yu, G. K. L. Wong, Y. Du, *Proc. Electrochem. Soc.* **1997**, *97–14*, 401 – 407; b) G. Gu, H. Huang, S. Yang, P. Yu, J. Fu, G. K. Wong, X. Wan, J. Dong, Y. Du, *Chem. Phys. Lett.* **1998**, *289*, 167 – 173; c) C. Hong, F. Ji-Kang, Z. Xin, R. Ai-Min, W. Quan Tian, J. D. Goddard, *THEOCHEM* **2003**, *629*, 271 – 277; d) E. Xenogiannopoulou, S. Couris, E. Koudoumas, N. Tagmatarchis, T. Inoue, H. Shinohara, *Chem. Phys. Lett.* **2004**, *394*, 14 – 18; e) H. Hu, W.-D. Cheng, S.-P. Huang, Z. Xie, H. Zhang, *J. Theor. Comput. Chem.* **2008**, *7*, 737 – 749.

[151] a) S.-I. Kobayashi, S. Mori, S. Iida, H. Ando, T. Takenobu, Y. Taguchi, A. Fujiwara, A. Taninaka, H. Shinohara, Y. Iwasa, *J. Am. Chem. Soc.* **2003**, *125*, 8116 – 8117; b) A. J. Perez-Jimenez, *J. Phys. Chem. C* **2007**, *111*, 17640 – 17645.

[152] P. Caravan, J. J. Ellison, T. J. McMurry, R. B. Lauffer, *Chem. Rev.* **1999**, *99*, 2293 – 2352.

[153] S. Laus, B. Sitharaman, E. Toth, R. D. Bolskar, L. Helm, L. J. Wilson, A. E. Merbach, *J. Phys. Chem. C* **2007**, *111*, 5633 – 5639.

[154] E. B. Iezzi, J. C. Duchamp, K. R. Fletcher, T. E. Glass, H. C. Dorn, *Nano Lett.* **2002**, *2*, 1187 – 1190.

[155] J.-J. Yin, F. Lao, P. P. Fu, W. G. Wamer, Y. Zhao, P. C. Wang, Y. Qiu, B. Sun, G. Xing, J. Dong, X.-J. Liang, C. Chen, *Biomaterials* **2009**, *30*, 611 – 621.

